DEGREE PROJECT

Electro polishing preparation of additive manufactured Ti-6Al-4V samples

Set the mechanic and electrolytic polishing parameters to get the best EBSD results

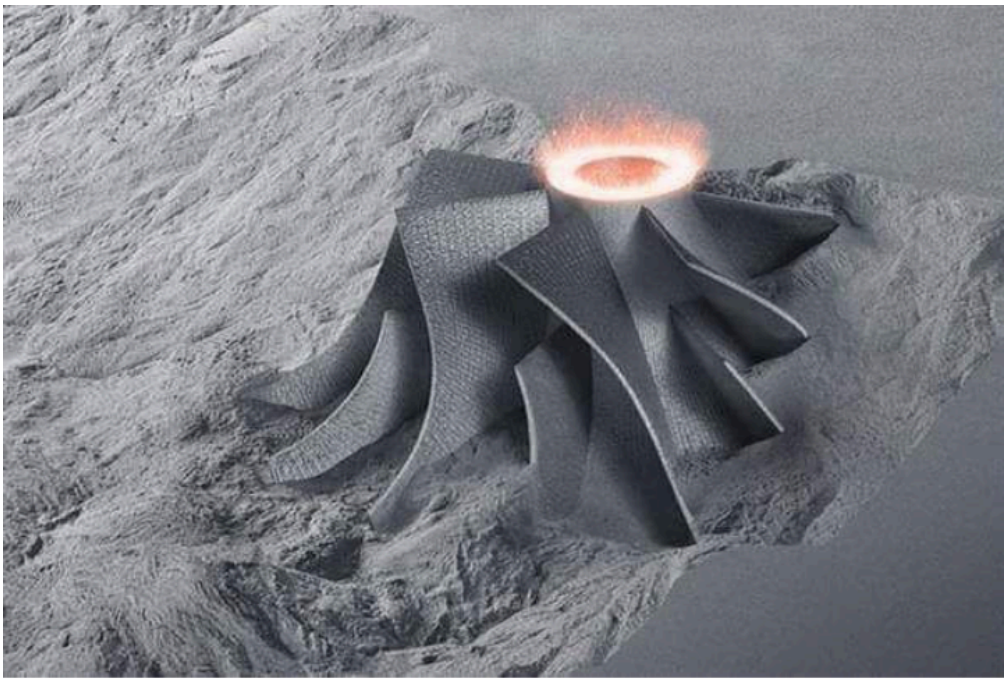

GABRIEL DIAZ GONZALEZ

Materials Engineering, bachelors level
2017

Luleå University of Technology
Department of Engineering Sciences and Mathematics

LULEÅ UNIVERSITY OF TECHNOLOGY

LULEÅ TEKNISKA UNIVERSITET

Universidad de Oviedo

Bachelor Thesis

Subject:

ELECTRO POLISHING PREPARATION OF ADDITIVE MANUFACTURED Ti-6Al-4V SAMPLES

Determination of the mechanical and electrolytic polishing parameters to get the best EBSD results

GABRIEL DIAZ GONZALEZ

Project course materials. T7023T
Supervisor: Magnus Neikter
Luleå University of Technology in collaboration with GKN Aerospace company
Engineering Materials
Material Science
Department of Engineering Sciences and Mathematics
Coordinador Universidad de Oviedo: María Jesús Lamela Rey

Fecha: 11/06/2017

Resumen en español del proyecto fin de grado

El objetivo de este estudio ha sido analizar los parámetros óptimos de tiempo y voltaje necesarios para conseguir un pulido óptimo mediante electro-pulido de muestras procedentes de diversos procesos de fabricación aditiva. En concreto se han analizado muestras creadas mediante SLS (sinterizado de laser selectivo) y LMpD (deposición de polvos metálicos fundidos por laser). Este pulido óptimo debía tener la suficiente calidad para asegurar un correcto análisis de la superficie de las muestras bajo microscopio electrónico SEM, utilizando la herramienta EBSD para su identificación micro estructural.

Las muestras analizadas estaban formadas por el mismo tipo de aleación, Ti-6Al-4V. Esta aleación presenta una serie de propiedades, tales como una buena resistencia a la corrosión, buen comportamiento de ductilidad, fatiga o una alta resistencia a la tracción, que la hace una de las mas utilizadas dentro de las aleaciones comerciales del titanio. Gracias a su bio-compatibilidad (no tóxica) es muy utilizada en aplicaciones médicas como implantes, prótesis…. Además su buen ratio de resistencia peso la hace idónea para la industria aeroespacial.

El Ti-6Al-4V es una aleación α-β. Presenta dos estructuras cristalinas estables dependiendo de la temperatura, α(HCP) and β(BCC). Cuando se desciende la temperatura desde la fase β por debajo de la temperatura de β_Transus, la fase α comienza a crecer en los bordes de grano de β. Cuanto mayor es el ratio de enfriamiento mas finas y largas son las laminas de α obtenidas. Por esto, esta aleación puede presentar distintos tipos de microestructuras, no obstante en las muestras analizadas solo se observaron dos tipos: estructura martensítica y de Widmanstätten (basket-weave). Esto es debido a que cada proceso de fabricación aditivo presenta diferentes ratios de enfriamiento dando lugar a microestructuras diferentes de Ti-6Al-4V con propiedades distintas.

Para la muestra de SLS (Sinterizado de laser selectivo) el ratio de enfriamiento es mas lento, luego su estructura es de tipo Widmanstätten. Se estableció una configuración en la maquina de electro-pulido de (20V,18s) de pulido y un grabado posterior de (14V,3s). Por otro lado, para la muestra de LMpD (deposición de polvos metálicos con laser) al ser el ratio de enfriamiento más rápido la microestructura observada fue de tipo martensítica. La martensita presenta mayor dureza pero es mas débil ante los procesos corrosivos, por lo que su comportamiento con el electro-pulido fue muy malo. Dificultando un pulido optimo al verse la muestra dañada por el ácido. Por ello se establecieron unos parámetros de electro-pulido de (20V, 10s) y sin grabado.

El proceso de preparación de las muestras ha consistido en un pulido mecánico mediante papeles de carburo de Silicio con diferentes precisiones, seguido de un tratamiento de electro-pulido como pulido final. Este tratamiento se ha efectuado mediante una maquina formada por un recipiente lleno de electrolito, donde se coloca un circuito eléctrico alimentado por una fuente de DC. Cuando la corriente fluye a través de la muestra (ánodo) a el cátodo su superficie es pulida mediante difusión iónica.

Para conocer los parámetros de control óptimos para preparar las muestras mediante electro-pulido hemos analizado las superficies tratadas con diferentes valores de tiempo y voltaje bajo microscopio óptico. Una vez obteníamos el pulido ideal, analizábamos el área tratada mediante SEM (microscopio electrónico), utilizando la técnica de EBSD (difracción de electrones retrodispersados) para ver las microestructura y las fases presentes en cada muestra. En el caso de la muestra creada mediante SLS, hemos observado una microestructura de tipo Widmanstätten con gruesas y cortas laminas de fase α creciendo en todas direcciones dentro de pequeños granos β. Por el contrario, la muestra LMpD ha presentado finas laminas de martensita creciendo a lo largo de grandes granos β (estructura martensitica).

Este proyecto ha sido realizado en el departamento de matemáticas y ciencias de ingeniería de la universidad de tecnología de Luleå, Suecia. Formando parte de una amplia investigación que esta institución esta desarrollando en colaboración con la compañía aeroespacial GKN para testear materiales, basados en aleaciones de aluminio, de piezas creadas por manufactura aditiva. Los cuales serán usados en el programa espacial del cohete Ariane. Por ello se hace imprescindible asegurar la calidad, predictibilidad y reproducibilidad de la aleación Ti-6Al-4V.

Comenzaremos esta investigación haciendo una introducción del Titanio, sus aplicaciones en la industria, propiedades mecánicas, cristalografía y sus aleaciones.

Posteriormente se profundizará en el estudio de la aleación Ti-6Al-4V usada en las muestras analizadas. Describiremos sus propiedades y el interés de su uso con manufactura aditiva (AM) en diferentes industrias, especialmente en la aeroespacial (debido a su buen ratio peso-resistencia) y médica (nula toxicidad). Entre los diferentes métodos de AM descritos, sólo se estudiaran el SLS (Sinterizado por Laser Selectivo) y el LMpD (Deposición de Polvos Metálicos calentados por Laser), considerando aspectos tales como sistema de alimentación (polvos o hilo), fuentes de energía (rayo de electrones, rayo X), defectos de manufactura…

En la parte teórica también se estudiará en profundidad el funcionamiento del tratamiento de electro-pulido como sistema de pulido final. Entrando a analizar los parámetros de control que se pueden regular para conseguir distintas calidades de pulido según el material a tratar.

Acabaremos esta parte exponiendo los principios de funcionamiento del SEM (microscopio de barrido electrónico), como colocar la muestra de manera adecuada y como debe configurarse el microscopio para conseguir que sus detectores obtengan la señal optima. De entre los diferentes detectores y métodos compatibles con el SEM, nosotros sólo usaremos el EBSD (difracción de electrones retrodispersados) del que obtendremos información sobre microestructura, identificación y orientación de fases presentes en las muestras.

En una segunda parte explicaremos el procedimiento experimental usado para desarrollar esta investigación. Describiendo materiales y maquinas usadas para preparar las muestras. Se demostrará que para el análisis bajo EBSD es mejor un pulido mecánico seguido de un electropulido final. Estableceremos los parámetros de voltaje y tiempo para conseguir la superficie optima de pulido. Y verificaremos cada prueba bajo microscopio óptico, hasta obtener una superficie espejo, característica de un buen pulido. Con la muestra perfectamente pulida en un área de su superficie, analizaremos dicha área bajo microscopio SEM y usaremos el EBSD para obtener información microestructural como ya vimos.

En la tercera parte de este estudio se exponen los resultados obtenidos. Es decir veremos como el tiempo y el voltaje hacían variar la calidad de pulido sobre la superficie tratada en cada una de las muestras. Y obtendremos los mapas IPF (Figura Polo inverso) sobre el área tratada mediante la técnica EBSD del microscopio SEM.

Para finalizar se proponen distintas mejoras y líneas de investigación alternativas que podrían desarrollar futuros estudiantes con el fin de mejorar o completar los resultados expuestos en este informe.

TITANIO

El Titanio es el cuarto material mas común en la tierra, pero su extracción es muy difícil por lo que su coste en el mercado es elevado. Esta presente en numerosas rocas ígneas y en los sedimentos derivados de ellas, también en muchos silicatos. Su campo de aplicación es muy variado, principalmente se usa en la industria aeroespacial y aeronáutica (50%), pero debido a sus propiedades también es usado en industria química, medicina, deporte o de generación de potencia.

En 1937 Justin Kroll desarrolla un método de producción industrial de Ti (Proceso Kroll) usado hasta nuestros días. Proceso consistente en la reducción del compuesto tetracloruro de titanio con magnesio molido, en una atmósfera de argón para evitar la oxidación.

El titanio presenta unas propiedades muy demandadas en las industrias antes mencionadas. Una buena relación resistencia-peso, un alto punto de fusión 1668ºC, baja capacidad de conductividad y dilatación térmica, una gran resistencia frente a corrosión gracias a la rápida oxidación y formación de su capa pasiva. No obstante por encima de 649ºC dicha resistencia baja considerablemente. El Ti no es tóxico, su alta biocompatibilidad lo hace el elemento idóneo para aplicaciones sanitarias como instrumentación médica, prótesis, implantes…El Ti puro presenta mucha ductilidad y baja resistencia a la tracción, pero estas propiedades pueden variarse con sus distintas aleaciones.

El titanio es un metal alotrópico que puede presentar dos tipos de estructuras cristalinas estables en equilibrio térmico: Fase α(HCP) and β(BCC). Este presenta una temperatura de transición entre una fase a otra de 882ºC, la cual puede cambiar mediante aleación. La relación entre ambas fases viene dada por Burgers.

El Ti puede ser aleado con hasta otros 30 elementos mediante sustitución átomos de Ti por otros o cubriendo espacios intersticiales. Esto es posible gracias al tamaño del diámetro medio del Ti. Existen tres tipos de elementos aleantes para el titanio: Estabilizadores Alfa (aumentan T transición beta), los Beta(eutectoides y isomorfos, disminuyen T transición beta) y los neutrales (no afectan a esta T). Atendiendo a estos tipos de elementos aleantes, se pueden crear diferentes tipos de aleaciones con el titanio. Estas aleaciones resultantes pueden clasificarse en: aleaciones Alfa, Beta y Alfa más Beta.

La aleación usada en este estudio (Ti-6Al-4V) es de tipo Alfa más Beta. Estas se caracterizan por tener entre un 5-40% de fase β a temperatura ambiente, sufren transformación martensítica al enfriarse rápidamente, mantienen un buen equilibrio entre ductilidad y resistencia y son tratables con procesos térmicos y de envejecimiento.

Ti-6Al-4V

Es la aleación de titanio más usada. Acaparando el 50% de la producción total de titanio. Es una aleación única gracias a sus excepcionales propiedades de resistencia, ductilidad, resistencia a la fractura y fatiga.

Aleacion	$s_{traccionys}$	s_{ys}	Limite impurezas %max weight				
			N	C	H	Fe	O
Ti-6Al-4V	900	830	0,05	0,10	0,0125	0,30	0,20

Es tratable tanto térmicamente como con procesos de envejecimiento. Se usa normalmente un recocido para obtener una buena relación resistencia, tenacidad, ductilidad y resistencia a la fatiga. Características también influidas por el proceso de enfriamiento y la composición química.
Así cuanto mayor es el contenido en oxígeno, nitrógeno, aluminio o vanadio, mayor es la resistencia. A menor contenido mayor: tenacidad a fractura, ductilidad, resistencia a la corrosión y velocidad propagación grieta.

Si se analiza la transformación de fase α(HCP) a β(BCC) mediante enfriamiento obtenemos que con un ratio bajo se obtiene una microestructura laminar de placas α (laminas largas y gruesas), tipo Widmasntatten, caracterizada por buena tenacidad, resistencia frente corrosión, resistencia a la fluencia y menor velocidad de propagación de la grieta. Además si se realiza un recocido de recristalización se mejora la ductilidad y la vida a fatiga. Por otra parte, ante un enfriamiento

rápido, las laminas α comienzan a ser cada vez mas cortas y finas hasta dar lugar a martensita (α', α'').

Debido a los factores vistos anteriormente, velocidad enfriamiento, pureza aleación o tratamientos térmicos o de envejecido, podemos obtener diferentes tipos de microestructuras para esta aleación. Se distinguen principalmente cuatro tipos: Equiaxial, Bimodal (Equiaxial y laminar), Martensítica o Laminar (Widmanstätten). En esta investigación sólo se estudiaron la martensitica y la laminar. La microestructura martensitica se consigue mediante un enfriamiento rápido o con un temple desde T mayor a T_ βtransus. Puede dar lugar a su vez a dos tipos de martensita: α', martensita acicular, hexagonal no termo-elástica (No puede darse en este tipo de aleación) y la α'', martensita ortorrómbica termo-elástica (propiedades de memoria de forma). Por otro lado, la microestructura Laminar o Widmastätten se obtiene a partir de enfriamiento lente desde una T mayor que la T_ βtransus hasta la region bifásica (α +β). A nuclea en los bordes de grano β, creciendo de forma laminar. Microestructura de tipo cesta, paquetes o colonias de gruesas placas de fase α y finas placas de fase β.

AM: MANUFACTURA ADITIVA:

El sistema de manufactura aditiva lleva usándose desde hace más de 50 años. En sus comienzos fue usado como sistema de prototipado pero hoy en día también se usa para la producción de series cortas. El principio de funcionamiento consiste en depositar material fundido siguiendo una trayectoria tridimensional marcada previamente. La deposición se produce capa a capa hasta conseguir el producto final. La pieza es previamente diseñada mediante un software de CAD, en la etapa de diseño también se definirán las secuencias de fabricación y los materiales a utilizar. Actualmente varias investigaciones tratan de mejorar aspectos tales como capacidad productiva y calidad obtenida bajo este proceso de manufactura. Actualmente, estos sistemas son compatibles con el uso de varios tipos de metales y polímeros, incluso a veces se pueden utilizar varios materiales al mismo tiempo. La manufactura aditiva en comparación con la tradicional es muy útil para hacer prototipado de piezas bajo demanda pudiendo obtener piezas de geometría compleja con diferentes escalas en un solo paso, ahorrando tiempo y espacio.

Los procesos AM más usados en la industria aeroespacial, según su fuente de calor:

- Fuente Laser: alimentación por hilo, por inyección polvos (LMpD) o en lecho de polvos (SLS)
- Rayo electrones: alimentado por hilo o por lecho de polvos
- Arco eléctrico (TIG): alimentado por hilo

Las muestras analizadas en esta investigación procedían de piezas fabricadas mediante LMpD y SLS.

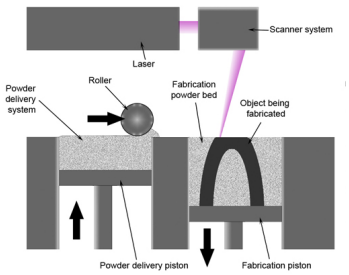

Fig 11. SLS[16]

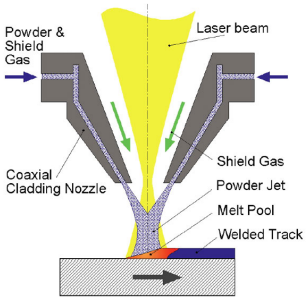

Fig 12. LMpD[19]

SLS (sinterizado por laser selectivo). Es un método de adición consistente en depositar una capa de polvo de unas décimas de milímetro en una cuba que se ha calentado a una T menor $T_{fusión}$ del polvo. Seguidamente un laser de pulso de alta potencia(CO_2) sintetiza (fusión y solidificación) el polvo en los puntos seleccionados. La cubeta desciende y se añade otra capa de polvo repitiéndose el proceso y creando la forma tridimensional deseada. Es una técnica de prototipado rápido y de

gran flexibilidad. Es muy útil para fabricar pequeños volúmenes de piezas que requieran buena funcionalidad. Permite fabricar modelos de geometría compleja. Inicialmente fue usado para prototipado, pero actualmente se esta empezando a usar en producción de tiradas cortas de piezas de uso final. Permite el uso de una gran cantidad de materiales como polímeros (nailon, poliestiresno…) o metales (acero, titanio, aleaciones…). El polvo a utilizar puede ser de un único componente o bicomponente (con polímeros). Dependiendo del material y el laser usado podemos alcanzar piezas con densidades del 100% del material, con propiedades físicas comparables a las fabricadas por métodos tradicionales. Permite seleccionar entre un fundido completo, parcial o sintetizado en fase liquida. No necesita soportes ya que la parte sinterizada está todo el tiempo rodeada de polvo. La información dimensional de la pieza proviene de un archivo informático previamente diseñado o escaneado.

En el LMpD se inyectan polvos de metal directamente sobre un haz enfocado de láser de alta frecuencia. No es necesario tener una atmósfera controlada (vacío o gases inertes). El polvo se va fundiendo y depositando sobre una base siguiendo una trayectoria marcada, generando así la pieza tridimensional. Procedimiento muy útil para la reparación de piezas y herramientas complejas imprimiendo sobre la propia pieza el metal que falta, en especial para piezas mecánicas móviles sometidas a desgaste. Permite fabricar piezas con distinta proporción de materiales diferentes entre unas zonas y otras. Las maquinas usadas son fácilmente escalables permitiendo la fabricación de piezas grandes, ya que no se requieren condiciones especiales ni la extensión de polvos sobre un lecho. La desventaja de este procedimiento es que no permite conseguir grandes precisiones porque no se tiene gran control sobre donde la deposición del material va a caer antes de ser fundido. Por lo que las piezas requieren normalmente de postprocesado.

ELECTRO-PULIDO:

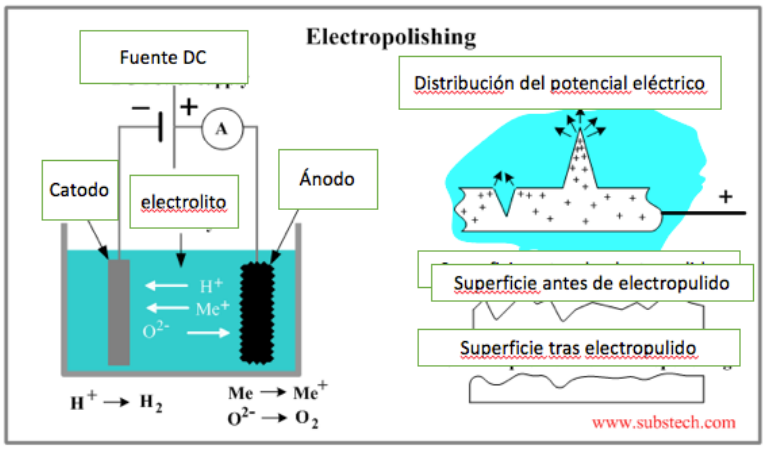

Fig 13. Electro-pulido[22]

Tratamiento superficial mediante el cual el metal a ser pulido actúa como ánodo (pierde e-) en una celda electrolítica, disolviéndose. Para ello se le aplica corriente que crea un film polarizado en la superficie tratada permitiendo la difusión de los iones metálicos. El espesor de la capa no es constante, siendo mayor en los valles (mayor R) lo que hace que los puntos altos de la superficie rugosa, picos, así como zonas con rebabas sean áreas de mayor densidad de corriente que el resto de superficies, lo que implica que se disuelvan a mayor velocidad. Esto da lugar a una superficie lisa, nivelada abrillantando la superficie tratada.

Para controlar este tratamiento tenemos varios parámetros de control, debemos conocer cuales son sus efectos para obtener la superficie con la mejor calidad posible. Estos parámetros son el área tratada, tipo de electrolito usado, el tiempo de exposición al tratamiento, la temperatura, el flujo del electrolito y el voltaje.

El espesor del material disuelto por este procedimiento varia entre las 10 a las 25 μm. Por lo tanto es claramente un tratamiento de pulido final. Previamente es necesario utilizar un pulido mecánico hasta alcanzar una calidad tratable con electro-pulido.
El electro-pulido mejora ciertos aspectos superficiales, como conseguir una superficie mas plana, eliminar rayones y micro-agujeros, evitando la acomodación de extraños elementos que originen procesos de corrosión localizada.

Si lo comparamos con el pulido mecánico, el electro-pulido permite tratar piezas con formas irregulares y de gran tamaño. Permite obtener resultados muy rápidos y facilita la labor de los operarios. Aumenta la resistencia a corrosión del metal tratado creando alrededor de él una capa de pasivación. Cuando usamos pulido mecánico obtenemos una superficie especular donde la luz refleja solo en una dirección. Está superficie además suele presentar deformaciones y daños superficiales a nivel microscópico, lo que dificulta su análisis bajo SEM y EBSD, tal y como comprobamos en este estudio. En el electropulido, la superficie es diferente, ya que si bien está libre de rayaduras y tensiones, presenta una estructura tridimensional que refleja la luz en todas direcciones, lo cual le da un aspecto satinado.

Atendiendo a los parámetros analizados en este proyecto (V,t) tenemos dos curvas características que nos definen la calidad del pulido obtenido en función de estos parámetros:

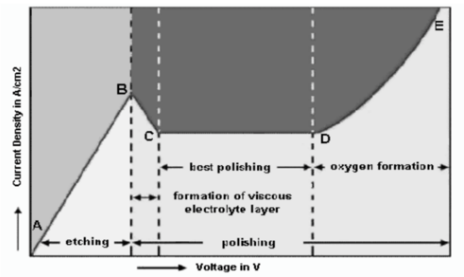

Fig 15. Curvas densidad corriente vs voltaje.[24]

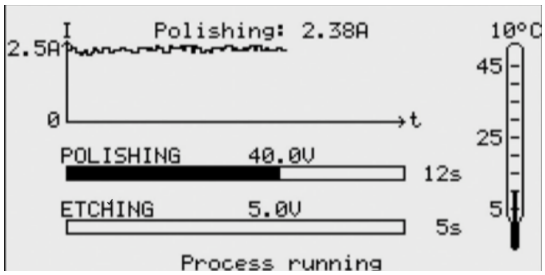

Fig 22/c. Curva densidad corriente vs tiempo [37]

Se pueden distinguir 3 regiones de funcionamiento:

A-B zona de ataque en que se trabaja para revelar los bordes de grano

B-C zona de formación de capa viscosa electrolítica

C-D rango donde mejor se puede producir el electro-pulido. En nuestro caso 19-21V

D-E Se puede obtener un pulido pero la excesiva formación de gas en la superficie de la muestra va a crear picaduras/defectos que empeora la calidad de superficie de la muestra y por tanto dificulta las caracterizaciones con SEM o EBSD

SEM: MICROSCOPIO ELECTRÓNICO DE BARRIDO:

Es una técnica donde un rayo de electrones bajo condiciones de vacío es enfocada hacia una superficie sólida de la muestra. Los electrones del rayo interactúan con los electrones de la muestra generando diferentes tipos de señal que pueden ser detectadas y analizadas obteniendo información sobre la topografía de la superficie de la muestra y su composición química. La magnificación que puede alcanzarse depende de la potencia del rayo de electrones que impacta sobre la superficie a analizar, pero esta puede alcanzar un nanómetro

Un rayo de electrones es lanzado desde la parte superior del microscopio (electrones primarios) sobre la superficie a analizar en nuestra muestra. Usaremos un campo eléctrico E para acelerar los electrones. Las lentes magnéticas son usadas para enfocar el rayo de electrones, obteniendo claras y detalladas imágenes del área a estudio. Una bobina permite dar una orientación correcta al rayo de electrones. Podemos ir cambiando dicha orientación para analizar distintos puntos de la superficie de la muestra. La muestra es colocada dentro de la cámara de vacío, asegurando que

esta permanece fija y no se dan vibraciones. El fino rayo de electrones impacta en un pequeño área de la superficie de la muestra, cuyos átomos interactúan con los electrones del rayo.

Asegurar una superficie con un pulido óptimo es esencial para obtener imágenes nítidas y poder realizar análisis fiables bajo un sistema tan sensible como es el SEM. Es por ello que en esta investigación hemos tratado de conseguir el mejor pulido posible para cada una de las muestras preparadas. Además también cobra gran importancia conseguir una buena señal captada por los detectores, para ello debimos orientar de manera correcta mediante uso de soportes la muestra y enfocarla bien.

El SEM esta equipado con diferentes tipos de sensores capaces de detectar las señales que los átomos de la muestra generan al interactuar con los electrones del rayo incidente. No obstante nosotros sólo utilizamos la técnica (o detector) conocida como EBSD.

EBSD: DIFRACCIÓN DE ELECTRONES RETRODISPERSADOS.

Es una técnica de caracterización micro-estructural cristalográfica para estudiar cualquier material cristalino. Con ella podemos obtener información sobre la microestructura, la orientación cristalina y las fases de la muestra analizada. Revelando textura, defectos, morfología de grano y deformaciones. El detector EBSD ubicado dentro del SEM esta formado por una pantalla de fósforo, lentes compactas y una cámara CCD de baja luz. Actualmente este sistema es capaz de analizar hasta 1800 patrones por segundo de señales provenientes de la muestra. Generando los mapas de polo inverso IPF(Figura de Polo Inverso, mapas de microestructura del área a analizar).

La muestra pulida es situada dentro de la cámara de vacío del SEM formando un ángulo de 70º con la horizontal respecto de la cámara de difracción. El rayo de electrones impacta sobre el área pulida a analizar. Algunos electrones son difractados (otros son absorbidos por la muestra) y pueden escapar del material, de entre estos, algunos colisionaran con la pantalla de fosforo excitándola y causando la fluorescencia. Los electrones difractados que colisionan con la pantalla tienen un ángulo cercano al ángulo de Bragg, estos forman sobre la pantalla bandas Kikuchi que corresponden al enrejado de difracción de los planos cristalográficos. Con tres bandas podemos definir la orientación del cristal respecto a una que se toma como referencia. Identificamos cada grupo de bandas con un EBSP (patrones de electrones retrodispersados), usando un modelo dinámico. Una vez tenemos identificados los patrones usamos un proceso de indexado mediante el cual definimos la orientación del cristal dentro del volumen de la muestra. Con el software del EBSD, los patrones de bandas son detectados matemáticamente usando la transformada de Hough. Los ángulos entre las bandas representan representan los ángulos entre los planos que conforman el enrejado de la microestructura. Por lo tanto, como ya vimos, cuando los ángulos entre tres bandas son conocidos una orientación es determinada.

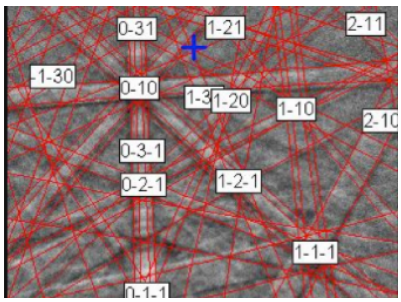

Fig 18. Identificación Kikuchi Bands [31]

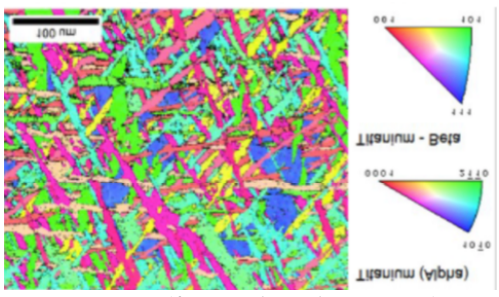

Fig 19. IPF (figura de polo inverso)[33]

A partir del EBSD podemos obtener los mapas IPF (figuras de polo inverso), estos mapas pueden describir espacialmente la orientación de los cristales dentro del material pudiendo examinar: la orientación del grano, los bordes de grano, la calidad del patrón de difracción, el tamaño de grano, la textura cristalográfica, la textura primaria de la fase original a elevada temperatura, las

tensiones residuales después de ensayos mecánicos, las agrupaciones de varias características microestructurales tales como precipitados y las fronteras de grano. Estos mapas están codificados en colores para ayudar a su interpretación. Para conseguir la orientación microestructural, usamos un eje como referencia y desde él establecemos el vector normal del plano de difracción cristalina para cada punto. Esta técnica permite estudiar la estructura de las colonias α a diferentes escalas. Desde ellas es posible reconstruir el grano β primario desde el que las microestructuras α provienen. Para conseguir esto, el software aplica la relación de Burgers sobre cada punto del área enfocada por el SEM, eligiendo la estructura de Burgers mas probable. Esta estructura estará dentro de las seis orientaciones posibles que el cristal α puede tener respecto el grano β primario.

PROCEDIMIENTO EXPERIMENTAL

Preparación de muestras:

Las muestras estaban previamente cortadas transversalmente a la dirección de deposición. Por lo tanto en cada una hemos escogido analizar la cara donde las microestructuras crecen en la dirección de deposición. Esto permite obtener una correcta identificación con el análisis EBSD.

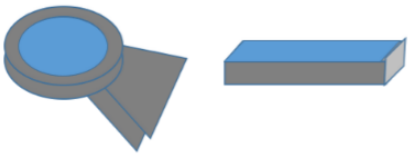

Fig20. Áreas seleccionadas para pulido de la muestra SLS izquierda y LMpD derecha.

Fig 21. Equipamiento de pulido mecánico con papeles de SiC

Antes del electro-pulido, hemos realizado un pulido mecánico para eliminar el material a nivel macroscópico. Hemos pulido con papeles de SiC con diferentes precisiones (comenzando por 1200 luego a 2000 y acabando con 4000). Para ello hemos usado la maquina semiautomática de pulido Metarserv 250.

Inicialmente hemos comparado la calidad superficial que podemos obtener con el electro-pulido en contraste con el pulido mecánico de alta precisión. En ambos casos realizamos un pulido mecánico previo con papeles de SiC como ya hemos descrito. Pero en el caso de un pulido muy fino usaremos Silicato coloidal (SiO_2). Es importante verificar que la muestra no presenta rayones o rugosidades mediante microscopio óptico. Antes de pasar de un grado de pulido a otro debemos de limpiar bien la muestra con agua. En la etapa final de pulido ya sea con pulido de alta precisión o electro-pulido es mejor limpiar la muestra con etanol.

Para realizar un pulido correcto de las muestras, debemos asegurar que la cara a pulir se encuentre paralela respecto al papel de SiC y evitar aplicar excesiva presión. Esto evitará que se creen diferentes planos sobre la superficie dando diferentes áreas de enfoque cuando realicemos el análisis bajo el SEM. Después de cada etapa de pulido se debe verificar que la superficie es plana y identificar la dirección de los rayones para pulir en la dirección perpendicular en la siguiente etapa. En nuestra investigación no se ha podido montar las muestras porque no hemos dispuesto de un material conductor, eléctrico, adecuado que nos permitiera usar el electro-pulido de manera óptima. Debido al pequeño tamaño de la muestra LMpD, fue muy difícil trabajar mediante pulido mecánico con esta muestra y conseguir resultados lo suficientemente precisos.

Electro-pulido:

Una vez obteníamos una superficie con una calidad superficial adecuada pasábamos a preparar la muestra mediante el tratamiento de pulido final, electro-pulido. Para ello usamos la maquina Lectropol-5 de la empresa Struers. La forma de utilización de esta máquina es: poner el recipiente con el electrolito dentro de la cavidad de la maquina. Seleccionar el soporte de plástico sobre el que colocaremos la muestra y que tenga el área de pulido adecuada para nuestra muestra. Colocamos la muestra y la ponemos en contacto con el brazo catódico.

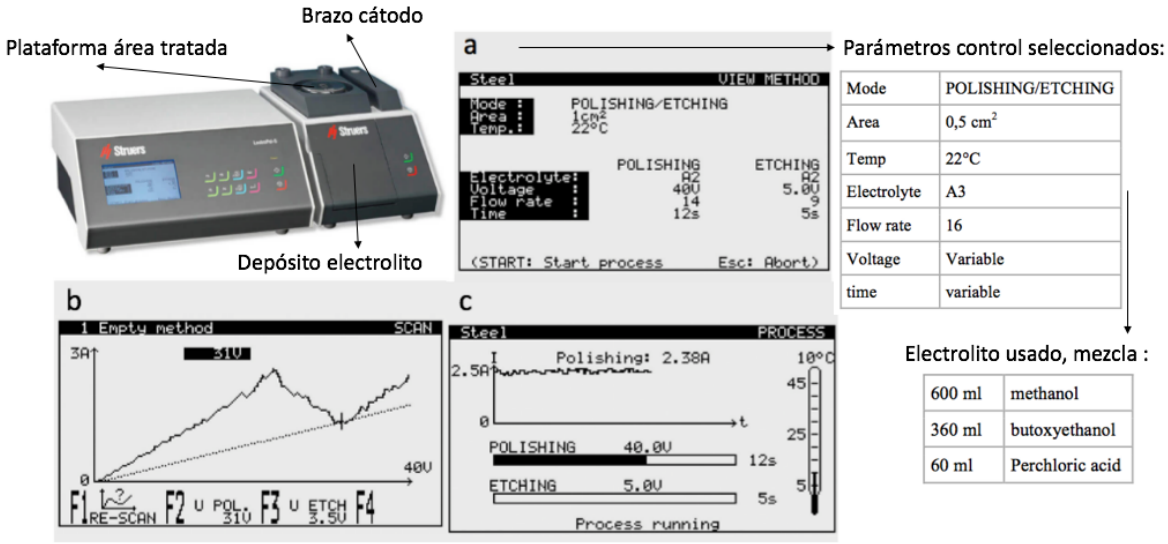

Mode	POLISHING/ETCHING
Area	0,5 cm^2
Temp	22°C
Electrolyte	A3
Flow rate	16
Voltage	Variable
time	variable

Electrolito usado, mezcla :

600 ml	methanol
360 ml	butoxyethanol
60 ml	Perchloric acid

Fig 22. Equipamiento electro-pulido. a)parámetros control. b)curva polarización. c)Curva densidad corriente respecto tiempo aplicación tratamiento [37]

En la figura 22.a podemos observar los parámetros de control que podemos variar para conseguir diferentes calidades de pulido. En este estudio solo nos hemos enfocado en conocer como afectan a dicha calidad, variaciones en el voltaje y el tiempo aplicados. Obteniendo así mismo los valores óptimos de estos parámetros que aseguraban un pulido adecuado para cada una de las muestras analizadas (SLS y LMpD). El área de pulido usada en ambos casos fue de 0,5 cm^2 debido al pequeño tamaño de las muestras. La temperatura ambiente estaba a 22ºC. El electrolito usado fue el Struers A3(mezcla facilitada por el fabricante, que preparamos cada cierto numero de pulidos por su desgaste) y el flujo se estableció a 16 (siguiendo la recomendación de la base de datos de Struers para titanio puro.

Con cada pulido el electrolito absorbe cationes metálicos hasta el momento en que su eficacia desciende, presentando un color amarillo. En este momento es necesario cambiarlo. Podemos comprar la mezcla directamente o hacerla nosotros como fue el caso, siguiendo la formula usada por Struers.

Para establecer el voltaje óptimo y conseguir el mejor pulido posible, la maquina tiene un escáner que nos da los voltios que nuestra muestra necesita. Este valor puede ser obtenida desde la curva de polarización Fig 22.b. Esta curva representa la densidad de corriente frente al voltaje aplicado. En ella podemos diferenciar tres etapas:

- Etapa 1: la corriente comienza a incrementarse según se aumenta el voltaje aplicado. Los cationes abandonan la superficie de la muestra y se difunden en el electrolito.
  $Ti \rightarrow Ti^{+2}+2e^-$
- Etapa 2: la corriente es casi estable aunque se incremente el voltaje. Comportamiento pasivo debido a la película anódica formada según la reacción:
  $Ti+4OH^- \rightarrow TiO_2+2H_2O+4e^-$
- Etapa 3: La corriente se incrementa de nuevo. Comportamiento traspasivo. El oxigeno es absorbido por la superficie del titanio. Los altos valore de densidad de corriente origina picaduras sobre la superficie

La fig 22.c representa la densidad de corriente respecto del tiempo. Para un voltaje fijado se ve como la densidad de corriente varia respecto al tiempo de aplicación del tratamiento. El fuerte salto que se ve al inicio de la curva podría ser debido a la capa de oxido pasiva formada sobre la superficie de la aleación del titanio. El enlace físico entre la capa de oxido y la superficie de la muestra es débil debido al efecto del metanol desestabilizando la película de oxido. Además

fomentar la reacción anódica origina fuerzas viscosas y turbulencias que favorecen la separación de la capa de oxido respecto la superficie.

Como comentamos previamente, la primera parte de esta investigación fue comparar el tipo de pulido obtenido mediante un pulido mecánico de alta precisión (papeles de SiC y un pulido final con Silica Coloidal) frente al método de electro-pulido (papeles de SiC con distinta precisión de pulido y un electro-pulido final). Como veremos en detalle en la parte de resultados, se pudo observar que con pulido mecánico nunca obteníamos buenos resultados de identificación mediante la técnica del EBSD antes descrita. Como comentamos anteriormente la superficie obtenida es especular, presentando un único plano sobre el que defracta el haz de electrones, a su vez los daños y las tensiones residuales consecuencia de un proceso mecánico hacia que esta opción la descartásemos desde un principio para preparar las muestras.

La muestra SLS mostró buen comportamiento frente a este tratamiento debido a que su microestructura laminar (debido a enfriamiento mas lento) presenta buena resistencia a la corrosión. Además aplicamos sobre ella un grabado a 14V y 3s que nos ayudaba a definir mejor el área tratada con lo que conseguimos mejorar los resultados de identificación mediante EBSD. Todo lo contrario ocurrió con la muestra LMpD, que presentaba una microestructura martensitica (debido a un ratio de enfriamiento elevado) que es débil ante los tratamientos corrosivos. En este caso no pudimos grabar la muestra porque se nos estropeaba mucho, y el electro-pulido debio realizarse con poco tiempo.

Para estudiar la influencia de los parámetros de control de tiempo y voltaje con la calidad en el pulido. Usamos la muestra de SLS. Estableciendo para cada experiencia un grabado de 14V y 3s. Para conocer como el tiempo de aplicación del electro-pulido afectaba a la calidad de pulido del área tratada establecimos un valor constante de voltaje (20V obtenidos de la curva de polarización) y mediante microscopio óptico fuimos observando las diferencias en el pulido según aumentábamos el tiempo (sin pulir, 5,9,18,25 y 60s). Por otro lado, para conocer como el voltaje aplicado varia la calidad en el pulido, establecimos un tiempo fijo (25s, el mejor tiempo para el análisis anterior) y mediante microscopio óptico fuimos analizando diferencias sobre la superficie variando el voltaje (sin pulir,5,20 y 45 V)

La tercera parte del estudio consistió en establecer para cada una de las muestras cuales eran los valores óptimos de voltaje y tiempo de aplicación del electro-pulido que aseguraban la mejor calidad de pulido posible y permitía obtener buenos resultados mediante la técnica de identificación de EBSD. Los valores del voltaje fueron obtenidos directamente de la curva de polarización, por lo tanto hicimos varios ensayos con cada muestra para establecer, analizando en cada caso bajo microscopio óptico, cual era el tiempo ideal.

Es importante reseñar que consideramos que un pulido es de calidad, cuando el área tratada no presentaba rayones, rugosidades y era totalmente plana (sin distintas caras de pulido). Una vez conseguíamos esto, limpiábamos la muestra con etanol para eliminar partículas y el electrolito corrosivo. A continuación secábamos la muestra con un secador para evitar las marcas del secado al aire. Tras acabar todo, se debía limpiar la maquina de electro-pulido siguiendo las instrucciones que esta indicaba (limpieza con agua y etanol), manteniendo el equipamiento en buenas condiciones.

Análisis bajo microscopio óptico:

Como se mencionó anteriormente, para realizar un análisis rápido de la calidad de pulido del área tratada usamos un microscopio óptico. En concreto utilizamos el modelo Microeclipse MA200 de la empresa Nikon. El proceso consistía en poner la muestra bajo el microscopio y conseguir un buen enfoque y iluminación sobre el área pulida. Si la calidad era suficiente podíamos pasar entonces a analizarlo con el SEM, en caso contrario debíamos volver a preparar la muestras cambiando los parámetros de control (grabado o sin grabar, voltaje y tiempo)

Análisis mediante SEM, EBSD y EDS.

Una vez teníamos una superficie correctamente pulida, la analizábamos bajo SEM. Para ello montábamos la muestra en un soporte de manera que esta mostrara 70º con la dirección horizontal a la plataforma. Para unir la muestra al soporte, podíamos usar pequeñas uniones atornilladas o pegado utilizando plata liquida. Lo importante era mantener la buena conductividad eléctrica. Poníamos el montaje dentro de la cámara de vacío y asegurábamos la correcta orientación de la muestra respecto el rayo de electrones y la pantalla de fosforo del EBSD. La finalidad era conseguir que el detector obtuviese la mejor señal posible de electrones difractados. Con el SEM buscábamos dentro del área pulida la zona que presentaba mejor calidad. Enfocábamos dicha zona y nos asegurábamos que la señal recibida por los detectores EBSD y EDS era suficientemente fuerte. Con el EBSD obtuvimos la fases, su proporción , orientación… mientras que con el EDS obtuvimos la composición química exacta de cada muestra (valores que no reflejamos en el informe porque no era objeto de este estudio).

DISCUSION DE RESULTADOS

Comparación de pulido mecánico frente a electro-pulido para usar con técnica EBSD

Para realizar esta parte preparamos la muestra de LMpD con un pulido mecánico previo consistente en papeles de pulido con varias precisiones 1200, 2000 y 4000. Después hacíamos el pulido maestro usando sílice coloidal durante varios minutos.

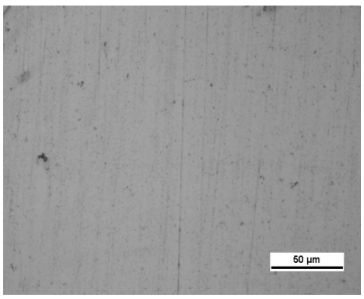

Fig23. a/ LMpD pulido con pulido mecanico con sílice coloidal

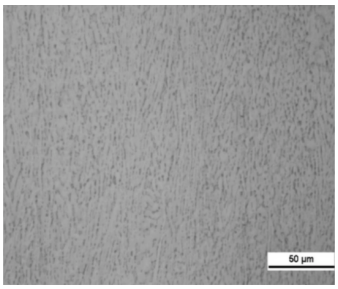

b/ LMpD pulido con electro-pulido con los parámetros optimos de pulido (20V,10s) y sin grabado.

Al tratar de analizar la muestra correctamente pulida con sílice coloidal mediante EBSD, no conseguimos obtener ningún resultado. Esto es debido a diferentes causas, algunas ya mencionadas anteriormente. El área pulida mecánicamente presenta diferentes propiedades en relación con la base del metal. Esta deformación es creada por fluencia consecuencia de las fuertes acciones mecánicas, el material de los picos es desplazado hacia los valles cubriéndolos y consiguiendo una superficie plana pero profundamente deformada. Este material superficial movido recibe el nombre de capa Bieldy y suele tener varios micrómetros de espesor. La superficie final es un estructura casi amorfa con inclusiones de óxidos y desechos del material pulido. Todo esto implica que las propiedades físicas y químicas de la superficie pulida sean distintas a las del metal base lo que origina tensiones mecánicas que puede dar comienzo a procesos corrosivos. Por otro lado, este efecto hace que sobre la superficie especular generada solo se refleje la luz en una dirección única.

Con el electro-pulido, la superficie pulida conserva las propiedades del metal de base. Cada elemento de la microestructura esta orientado en una dirección y cuando el rayo de electrones impacta en la muestra, los e^- son difractados en varias direcciones. Obteniendo buenas identificaciones mediante EBSD. Por lo tanto en las experiencias posteriores decidimos usar una combinación de pulido mecánico (para eliminar gran parte del material), seguido de un electro-pulido para conseguir la calidad requerida.

Variación del voltaje y el tiempo para ver la calidad de pulido obtenida mediante electro-pulido

En esta parte hemos usado sólo la muestra SLS de la aleación Ti-6Al-4V. Como ya habíamos explicado, se observaron diferentes calidades de pulido obtenidas con distintas configuraciones de tiempo y voltaje de electro-pulido. Estas observaciones se realizaron rápidamente bajo microscopio óptico.

Parámetros de control introducidos en la maquina de electro-pulido: (Struers Lectropol-5)

<table>
<tr><td>Modo</td><td>Pulido/grabado</td><td colspan="2">Resultado del voltaje optimo de la curva de polarización</td></tr>
<tr><td>Área</td><td>0.5 cm^2</td><td rowspan="6">Pulido: 20V

Grabado: 14V</td><td rowspan="6">Efecto borde:
 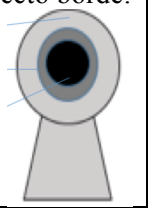 </td></tr>
<tr><td>Temperatura</td><td>22ºC</td></tr>
<tr><td>Electrolito</td><td>A3</td></tr>
<tr><td>Caudal de flujo</td><td>16 (recomendado por Struers para Ti puro)</td></tr>
<tr><td>Voltaje</td><td>Variable</td></tr>
<tr><td>tiempo</td><td>Variable</td></tr>
</table>

Hemos utilizado un grabado a 14V y 3s, porque la curva de polarización nos dio esta recomendación y porque un grabado define mejor la microestructura, dando mejores resultados mediante la técnica de EBSD.

Para ver el efecto del tiempo respecto la calidad del pulido, hemos establecido el voltaje a 20V (recomendado por la curva de polarización) y hemos ido cambiando el tiempo: sin pulido, 5, 9, 18, 25s y el extremo en 60s). Para ver el efecto del voltaje, establecimos el tiempo a 25s, el tiempo que mejores resultados nos dio en el análisis anterior, y fuimos cambiando el voltaje: sin pulido, 5, 20V y el extremo en 45V).

En la muestra de SLS se ha dado el Efecto de Borde. Este efecto es caracterizado por presentar un campo eléctrico mayor en los bordes del área pulida que en el centro. Por ello los bordes están muy pulidos mientras que el centro presenta un pulido más pobre. En el medio del área pulida, la capa de óxido permanece parcialmente, esto hace que el pulido no fuera completo. Cuando limpiamos dicho área con etanol podemos observar la superficie rugosa. Como explicaremos mas adelante con altos voltajes el Efecto de Borde decrece, pero la superficie puede mostrar grietas y fisuras.

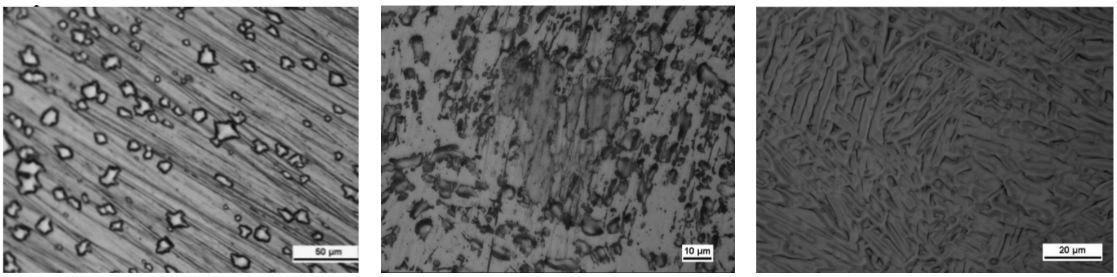

SLS sin pulido 0s *5s de pulido* *25s de pulido*

Tabla 9. Influencia del tiempo de electro-pulido. 50x
Grabado: 14v 3s. Voltaje constante a 20V

Cuando aplicamos tiempos cortos se muestra un pulido muy pobre debido a que la capa de oxido no ha sido del todo separada. No obstante, si aumentamos el tiempo del tratamiento podemos mejorar el área pulida, eliminando parcialmente la capa de óxido de la superficie. Con el tiempo adecuado (25s en nuestra muestra) podemos llegar a obtener una superficie pulida y suave. No obstante si la duración del electro-pulido es muy larga (60s) aparecerán rupturas y grietas sobre la superficie. Obteniendo áreas muy pulidas donde la concentración corrosiva será mayor y otras que aún conserva la capa de oxido protectora. En resumen, cuando aumentamos el tiempo de pulido hasta los 25s, los rayones y las rugosidades desaparecen. Después de ese tiempo, no se obtienen grandes mejoras pero si lo aumentamos mucho (60s), la superficie presentará damos como grietas y rugosidades.

En esta investigación se ha usado una aleación de titanio, por lo tanto la disolución podría ser mayor en algunas micro-regiones debido a la existencia de pares galvánicos. Dos metales en contacto en un medio húmedo, el metal mas noble será menos reactivo que el metal más inerte. Es decir, el metal mas reactivo se desgastará más rápidamente. En nuestra muestra el titanio es un metal mas noble que el aluminio.

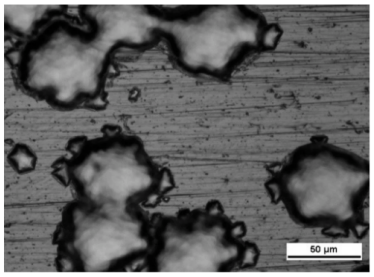

SLS pulido a 5v

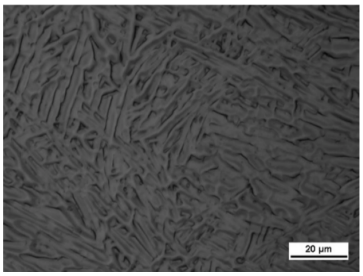

SLS pulido a 20V

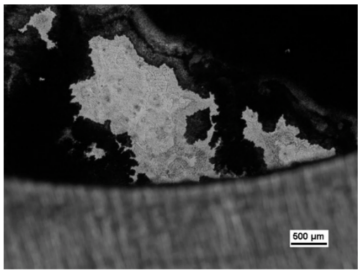

SLS pulido a 45V. 2.5x

Tabla 10. Influencia del voltaje con la calidad de pulido.
Grabado: 14V 3s. Tiempo constante a 25s

Con bajos voltajes, por debajo de los 15V, el electro-pulido es sólo efectivo en áreas cercanas a los bordes del área tratada (Efecto Borde). La capa de óxido no consigue desprenderse de la superficie y por tanto el pulido en el centro es pobre. Con el voltaje óptimo, el obtenido a partir de la curva de polarización, se consigue suministrar suficiente densidad de corriente para obtener una superficie pulida suave y el efecto borde se mitiga. Con altos voltajes la situación cambia de nuevo, en algunas zonas la capa de oxido es despegada, luego la corrosión actúa más intensamente y el pulido es muy alto, pero solo en esas zonas. En otras la capa de oxido se quema pero no se desprende. Esto da lugar a hoyos y grietas sobre la superficie.

Otro aspecto a considerar es que no estamos tratando con titanio puro sino con una aleación. De forma que habrá zonas con distintas resistencias a la corrosión. Las áreas donde los elementos de aleación estén en mayor concentración, serán mas débiles y sufrirán mayor corrosión.

Parámetros de electro-pulido para conseguir pulido óptimo.

Para preparar la muestra SLS , de la forma que obtuviéramos el mejor pulido posible para analizar su microestructura bajo EBSD, hemos comenzado con un pulido mecánico a 1200 con papeles de SiC, luego hemos mejorado el pulido pasando a 2000.

Para realizar el electro-pulido hemos establecido los parámetros de control como se describió anteriormente: área 0.5 cm^2, temperatura ambiente a 22ºC, electrolito A3, caudal de flujo del electrolito a 16 (valor recomendado por Struers para Ti puro). Tras lanzar un escaneado de la superficie a pulir mediante la máquina de electro-pulido, la máquina recomendó usar un valor de 20V para el pulido y 14V para el grabado. Por ultimo, tras probar con varios tiempos se estableció que la mejor superficie pulida se obtenía con un pulido durante 18s y un grabado de 3s.

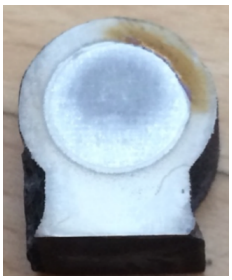

Fotografía de la muestra SLS

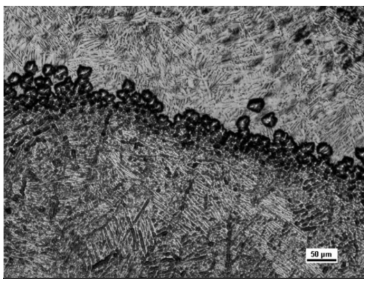

Micrografía bajo microscopio óptico. 20x

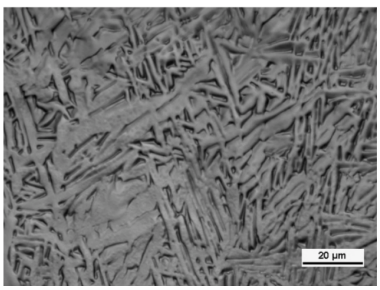

Micrografía del área más pulida cerca de los bordes. 50x

Tabla 11. Pulido óptimo con electro-pulido de la muestra SLS

Para la muestra LMpD realizamos también un pulido mecánico previo comenzando con un papel de SiC de 1200, luego 2000 y acabando con el de 4000. Tras establecer los mismos parámetros que para el caso de SLS excepto en el voltaje y el tiempo, se lanzo el escáner y de la curva de polarización obtenida establecimos un pulido a 20V. En este caso la curva no recomendó realizar un grabado. Además tras evaluar varios tiempos, observamos como esta muestra presentaba gran debilidad frente a la corrosión del electrolito. Por lo que como máximo pudimos tratarla durante 11s antes de que se dañara la muestra.

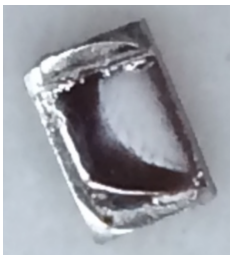

Fotografía de la muestra LMpD

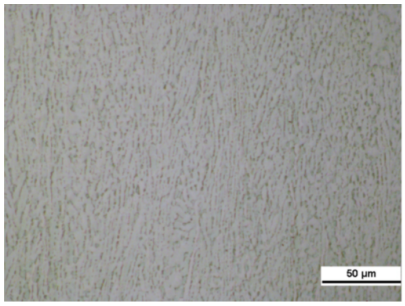

Micrografía LMpD 50x

Tabla 12. Pulido óptimo con electro-pulido de la muestra LMpD

Si comparamos los procesos de manufactura aditiva utilizados para cada una de las muestras, el LMpD muestra un ratio de enfriamiento mayor que el SLS. Esta rapidez de enfriamiento da lugar a una microestructura de tipo martensitica (α´´, martensita ortorrómbica termo-elástica). La fase martensitica es como la fase α, pero con laminas mas finas. Esta fase es magnética, con moderada resistencia a la corrosión pero un alto limite elástico. A causa de esto, la muestra mostro una gran sensibilidad con el electro-pulido. La capa de óxido se disolvió mas rápido en el electrolito, dejando la superficie al descubierto en contacto con este durante más tiempo. Por ello finalmente establecimos no usar el grabado y aplicar solo 11s de tratamiento, más tiempo implicaba dañar la superficie con grietas, agujeros y rugosidad.

Hay que hacer mención especial también, a la dificultad que implico trabajar con una muestra tan pequeña. Tratamos de utilizar algún tipo de recubrimiento para poder trabajar mejor con ella, pero no dispusimos del material conductor adecuado que nos permitiera realizar el electro-pulido con la suficiente precisión.

Análisis de las muestras mediante SEM con la técnica de EBSD

Mediante distintos sistemas de montaje colocábamos las muestras formando un ángulo de 70º con la plataforma horizontal, dentro de la cámara de vacío. Luego, lanzábamos el rayo de electrones sobre el área pulida de la muestra. El objetivo aquí era establecer la orientación de la muestra adecuada y los parámetros del rayo de electrones tal que el detector EBSD captara la mayor intensidad de señal posible. A su vez debíamos asegurar un enfoque perfecto del área seleccionada para el estudio. Una vez teníamos enfocada dicha área, lanzábamos el programa Aztec activando los detectores del SEM explicados anteriormente; EBSD y EDS

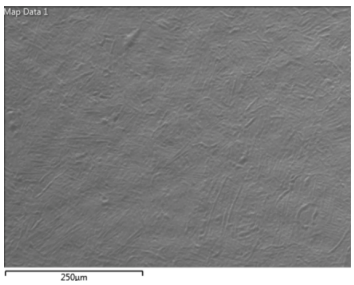

Area enfocada SEM de SLS

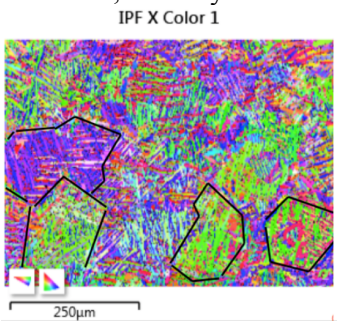

Mapa IPF

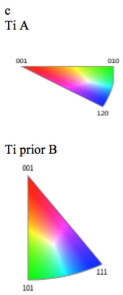

triángulos orientaciones

Tabla 13. Análisis bajo SEM con EBSD de la muestra SLS

El análisis EBSD de la muestra SLS se efectuó durante 20h, usando una precisión normal, hasta que el sistema escaneo todos los puntos del área seleccionada. El software compara las bandas Kikushi obtenidas con las que tiene en su base de datos y desde una dirección de referencia <001> el sistema identificaba las direcciones de los planos cristalinos dados en la microestructura. A

cada vector normal de un plano microestructural se le daba un color que indica su orientación. Es así como se forman los mapas IPF (Figura de Polo Inverso).

En la tabla 13 podemos observar laminas de α dentro de granos primarios β creciendo en forma de enrejado de cesta característica de la microestructura de Widmanstätten. Como se observa en los mapas, los bordes de grano de β primario, son fácilmente identificables. Los triángulos de colores muestran las orientaciones cristalográficas de cada fase. El triangulo de la fase β primaria es obtenido a partir del de fase α utilizando la relación de Burgers.

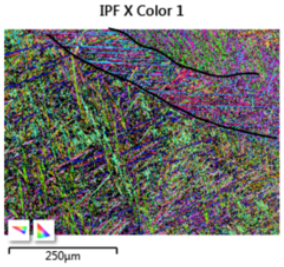

Tabla 14. IPF del área pulida de muestra LMpD

En el caso de la muestra de LMpD el mapa IPF, del área pulida enfocada por el SEM con el análisis EBSD, muestra claramente una estructura martensitica. Con enormes granos β creciendo en la dirección de enfriamiento. Dentro de ellos encontramos finas laminas de martensita (α'') creciendo en la misma dirección.

CONCLUSIONES Y RECOMENDACIONES EN INVESTIGACIONES FUTURAS.

- El pulido mecánico aunque puede conseguir resultados de gran precisión, no es el más recomendable para preparar muestras con la finalidad de analizarlas mediante SEM y EBSD. Este proceso crea daños a nivel microscópico deformando la microestructura del metal base.
- Si aplicamos poco tiempo el tratamiento de electro-pulido, la capa de oxido no se llega a desprender y el pulido final es escaso. Si aplicamos el tratamiento el tiempo adecuado, la capa de oxido se va quitando y se obtiene una superficie espejo, lisa y suave. Si el tiempo es muy alto aparecerán agujeros y grietas en la superficie, además de crearse micro-rugosidades por efecto de los pares galvánicos.
- Si aplicamos voltajes bajos, aparece el Efecto de Borde, donde los bordes están mas pulidos que el centro, donde la capa de óxido no ha conseguido desprenderse. Si aplicamos el voltaje optimo con electro-pulido, se quita la capa de oxido y hay un pulido uniforme en toda la superficie. Con altos voltajes, aparecen zonas con capa de oxido y otras muy pulidas creándose agujeros y grietas
- Los parámetros óptimos, de electro-pulido, para la muestra SLS han sido un pulido 20V y 18s y un grabado posterior a 14V y 3s. Mientras que para la muestra de LMpD ha sido un pulido de 20V y 11s sin aplicar grabado. La estructura martensitica del LMpD mostro mal comportamiento frente a la acción corrosiva del electrolito.
- La muestra SLS mostro muy buenos resultados de identificación micro-estructural mediante EBSD son un 92.18% de Ti-Hexagonal- α, un 0.85% de Ti-cubico- β, y un 6.97% de soluciones no identificadas. Cabe destacar que el sistema no fue capaz de distinguir entre fase α y martensita. La muestra LMpD presento resultados mucho peores, con un 35% del área sin identificación y el resto como fase α. Aunque en verdad es martensita, tal y como se puede observar en su mapa IPF con laminas finas creciendo en dirección de los largos granos β.
- Por ultimo mencionar algunas mejoras que se podrían realizar para continuar con esta investigación. En primer lugar se aconsejaría no trabajar con muestras muy pequeñas o de hacerlo poder montarlas con un material conductor de la electricidad. Para muestras con martensita, que presenta poca resistencia ante corrosión, recomendaríamos un proceso previo de envejecido o un tratamiento térmico que mejore sus propiedades. Hacer un ataque químico abrasivo y compararlo con los resultados del electro-pulido. Comprobar como varía la calidad del pulido si alteramos otras variables de control como la temperatura, el flujo del electrolito, el tamaño del área a pulir o usando otro tipo de electrolito. Realizar mismo estudios con muestras provenientes de otros procesos de manufactura aditiva y convencional. Analizar la muestra LMpD mediante la maquina de difracción de rayos X (XRD), la cual permite distinguir entre fase α y martensita.

CONTENTS

ABSTRACT

In this project we have analysed the Ti-6Al-4V alloy. This alloy has interesting properties such as good corrosion resistance, exceptional behaviour of ductility, fatigue and tensile strength [6]. It is non toxic, so it is developed to use in a variety of medical applications. Moreover, because of its good strength to weight relationship, it is useful in aerospace industry [2]. The Ti-6Al-4V is an α-β titanium alloy. It presents two stable crystal structures depending the temperature, α(HCP) and β(BCC). When we decrease the temperature from the β phase below the β Transus temperature, the α phase begins to grow into β boundaries. With a high cooling rate, we obtain short and thin α lamellas otherwise long and thick lamellas. This alloy presents several types of microstructures but for our research the most important are martensite and Widmanstätten (basket-weave) [7]

In this research, we have analysed two samples made by additive manufactured, SLS (Selective laser sintering) and LMpD (Laser Metal Powder Deposition). It is important to note that the cooling rate in the SLS process is lower than in LMpD, this explains why the samples showed different microstructures [12]. The aim of this project have been set the optimal polishing parameters for each sample in order to get the best EBSD (Electron backscatter diffraction) results. For the SLS sample, we have set a polishing (20V, 18s) and an etching (14V, 3s), and for the LMpD sample a polishing (20V, 10s) but no etching. This is because the LMpd has a martentitic structure with a low corrosion resistance. [13]

The process of the sample preparation has consisted in a mechanical polishing by SiC papers of different accuracies, followed by an electro-polishing. This surface treatment includes a container full of electrolyte, where we put an electric circuit supplied by a power source. When the current flows through the sample (the anode) to the cathode its surface is polished by ionic diffusion [39]. To know the correct control parameters, we have played with variations of time and voltage to analyse its relation with the final surface quality. After each experience, we have checked the polishing results by optical microscope. To conclude this project, we have analysed the polished area by electron microscope (SEM) and EBSD to see the microstructure and phases exhibited in each sample. In the case of SLS sample, we have found thick and short lamellas of α phase growing in all directions inside small β grains (Widmanstätten microstructure). Furthermore, the LMpD has presented thin lamellas growing along big β grains. (Martensite)[7]

ACKNOWLEDGEMENTS

I would like firstly to thank the Department of Engineering Sciences and Mathematics staff for giving me the opportunity to learnt a lot of things and always help me when I have encountered some difficulties during the develop of this project. Thanks to my friends and colleges to do more pleasant the work, in special to Rosa for her good advices and her friendliness. And I would particularly like to thank my supervisor, Magnus Neikter, for its patient and readiness. Assisting me wherever possible, always answering my questions and encouraging me when the results from the tests were not quite satisfactory.

INTRODUCTION

Commercializing additive manufacturing of titanium can be the future of the manufacturing due to lowering the cost and losses material during manufacturing process [2]. This project was realized to the course T7023T: Project course Materials belonging to engineering sciences and mathematics department. This report take part in a large investigation between Luleå University of Technology and GKN Aerospace company to test materials, based in Ti alloys, of additive manufactured which will be used in the Ariane rocket program. So it is fundamental to ensure the quality, predictability and reproducibility of Ti-6Al-4V4 material.
In the course of this project, we will discuss issues cutting across titanium and its alloys, specially Ti-6V-4Al alloy. We will begin by talking about the origins of titanium, its history, the properties and the interest of the industry, the crystallography and the possible alloys. Then we will focus in the Ti-6Al-4V alloy, discussing its properties related to the additive manufactured and the industrial uses, in particular in aerospace and medical applications. Among the several AM processes, we will only discuss methods SLS and LMpD, considering aspects such as feed material (wire or powder), energy sources (electron beam, X-ray), manufacturing defects…
In the second part of this report, we will explain the methods used to prepare the samples. We will demonstrate the suitability of mechanical polishing and electro-polishing to get the best polished surface. We will see how we can analyse the microstructure of the samples by optic and electron microscope. We use the optic microscope to check the surface quality, evaluating differences with different polishing parameters (time and voltage). Then we will explain how to scan a polished area by electron microscope to identify microstructures (SEM), considering aspects such as functioning principles of SEM and EBS, orientation of the sample or steps to focus the area selected with the best quality. From the SEM and EBSD we obtain information about the microstructure, identification and orientation of the phases.

1 TITANIUM

1.1 Introduction to Titanium

Titanium is the fourth most common abounded material in the earth. But it is expensive because it is complicate to produce. We can find it inside numerous igneous rocks and in their sediments. It is also present in many silicates. The minerals that show the biggest concentration of this metal are the Rutile (TiO_2) and the Ilmenite ($FeO \cdot TiO_2$)[1]. Respect to the economic approach, one industry with a few companies works in the titanium extraction and its commercialisation, mainly sited in Germany and Russia. So the price of this metal is very sensible to the economics cycles. The Titanium demand in the market remain almost constant with an annual growth rate of 9%. During the international recession there was a decrease in price. But in the recent years it has recuperate its value and nowadays it is considered one of the most promising material for future applications. Typical applications of the Titanium and its alloys: [2][3] Aerospace and aeronautic industry (50%), architecture, chemical industry, medicine, sport, power generation
In 1971 William Gregor, British mineralogist and chemical, discovered the Titanium from the magnetic sand in the Helforf river, England. He obtained this metal by isolating of the ilmerite. In 1795 Martin Heinrich Klaproth observed Ti in a rutile sample. In 1910 Matthew Albert Hunter obtained Ti with a high purity degree (99,9%), by "The Hunter process" invented by himself in the Rensselaer Polytechnic Institute in Troy, New York. In 1937 Wilhelm Justin Kroll, mineralogist, developed an industrial method to produce Ti. The "Kroll Process" has been used until the present. it consists in a reduction of titanium tetrachloride and magnesium grounded in an Argon atmosphere to avoid the oxidation. Several time after other method was developed to get pure Ti for research by decomposition with the help of iodine

1.2 Applications in industry

In the industry the Titanium plays an important paper. It is used to weld pipes, in the heat exchanges and to make Irisdescent glass and smokescreens from TiO2. A cause of its hardness and corrosion resistance, it is useful in petrochemical applications and in the paper industry. We can apply the Ti by ultrasonic welding and by wave.
In the Aerospace and aeronautic industry, it is used in several applications thanks to the good properties that presents, such as; High proportion of breaking load and density, high corrosion resistivity, fatigue resistivity, high temperature resistivity without deformation. For this, it is applied in aviation, spaceships, ships, missiles, engine component and desalination plants or equipment in contact with sea water.
The titanium is no toxic, so it is used in multiple applications thanks to its biocompatibility. It is used with surgical tools, medical implants with a life of around 30 years. Due to the Titanium is not a ferromagnetic material, the patients with this implants can use the magnetic resonance. We have focused our research in the alloy of titanium Ti-6%AL-4%V that shows a low elastic constant very similar to the human bones which have a good charges distribution. However, this material presents more rigidity, so it suffers more damage
In the automotive sector, a key factor is to reduce weight while the resistance and the rigidity don´t change it. The high price of titanium causes that only the models of high quality use this material.
We can found Ti in sport world too. Tennis rackets, golf clubs, bicycle frame, helmets, horseshoe, cooking tools and equipment for the mountain are made from titanium. They are more expensive but offer more hardness and resistance in relation with their weight.
In the military field the Ti is a widely used with weapons, cases for portable computers, covering submarines…
Thanks to its durability, inert properties, water resistance and anti-allergic, the titanium is the element ideal to use with jewels and complements. Though ionisation we can cover the titanium items with a passive layer of oxide that protect the material
On the other hand, we can found the Ti in several statues and buildings around the world. Some examples are the Memorial statue of the first cosmonaut in make a space trip (40 metres high), Yuri Gagarin(Moscow), the covering of the Guggenheim museum (Bilbao, Spain), Cerritos Millennium Library (Cerritos, California), Frederic C.Hamilton Denver (Colorado) and the Monument for conquers of the space (Moscow).
It is used in waste containers, specially with nuclear wastes, due to its strong corrosion resistance. So it plays an important paper in chemical and power generation.
The Ti is combined with steel alloys to reduce the crystallinity (deoxidant) and with stainless steel to descend carbon proportion. It can be combined with other metals such as aluminium, vanadium, copper… In our case we have analysed the alloy Ti-6Al-4V [2]

1.3 Properties

Very good relation strength to weight ratio, high melting point (1668°C), poor thermal conductivity and density higher than aluminium but lower than steel. It is very useful in aerospace industry because its strength is similar with regard to steel alloys
There is an interest in the additive manufacturing to reduce the buy-to-fly ratio of the titanium alloys. The Buy-to-Fly ratio is the weight ratio between the raw material used for a component and the weight of the component [5]. There is an interest in the research about Ti alloys because of its high market price and high machining costs. Ti has excellent corrosion resistance because of an external passivation layer is formed almost instantaneously upon contact with oxygen, preventing diffusion of oxygen with the metal underneath. This layer is more resistant than the aluminium passivation layer [8]. Over 649º the oxidation resistance decrease very quickly. So the contact with O2 or the N2 of the air (or other gases) can debilitate it. Ti alloys present better resistance against pitting under normal working conditions. It is important to state that the Properties of Ti can be changed through specific alloying. [8]

Atomic number	22
Atomic weight	47.90
Atomic volume	10.6 cm^3/mol
Covalent radio	1.32 A=0.132 nm
Density	4.51 g/cm^3
Welding point	1668 ± 10ºC
Boiling point	3260ºC
Specific heat	522 J/kgK
Thermic conductivity	11.44 W/mk
Latent heat of fusion	440 KJ/kg
Latent heat of vaporitation	9.83 MJ/kg
Hardness	100 HV
Tensile strength	240 Mpa
Yield strength	115 Gpa-120 Gpa
Poisson coefficient	0.33-0.361
Thermic expansion coefficient	$8.41 \cdot 10^{-6}ºC^{-1}$
Electric conductivity	3% IACS* (where Cu=100% IACS*)
Electric resistivity	420 nΩm

Table 1. properties of elemental titanium[6]
**IACS: International Annealed Cooper Standar*

If the titanium is pure, it has a low tensile strength, so a high ductility. In the Ti alloys these properties can be changed. In general, when the oxygen and the nitrogen appears dissolved in the titanium lattice, the resistance raises. However, if these elements are in oxides form, the contrary effect happens. [8]
Titanium is not toxic and it can´t be absorbed into the body. So it is used with several medical applications such as prosthesis and surgical equipment. Although, several studies show that the titanium can be absorbed into the tissues that contains silica (e.g nails). Some vegetables or fungus use the titanium like a nutrient. So we can use these organisms to bio-convert and clean places contaminated with this metal. [4]. The metallic shavings or the powder of titanium are very flammable. The suspension particles can explode under conditions of high pressure or temperature. In case of the fire created by titanium particles, it is necessary to use class D extinguisher. Ti can be burned if we put in contact one zone unoxidised (galvanic layer) with liquid oxygen.

1.4 Crystallography

Titanium is an allotropic metal that can appear in two types of stable crystal structures in thermal equilibrium:

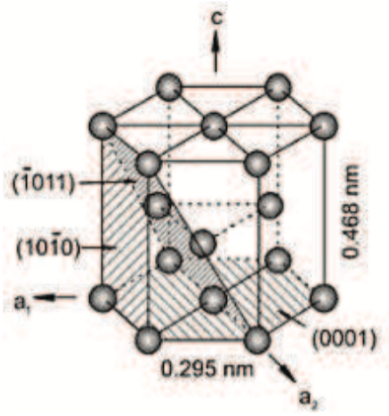

fig1.Crystal structure Ti α HCP[7]

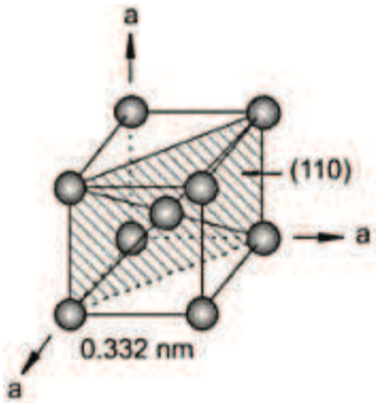

fig2. Crystal structure Ti B BCC[7]

In the figure 1 is represented the α phase, hexagonal close-packed (HCP). In this phase the planes more densely packed are (0001) basal plane, (1010) one of the the three prismatic planes and plane (1011) one of the six pyramidal planes. The maximum packet direction is <1120>. This phase is characterised by lattice constants a=0,295 nm and c=0.468 nm. The α phase (HCP) has higher packing factor than B (BCC). Furthermore, the figure 2 represents the β phase, body centred cubic (BCC). Where the plane more densely packed is (100), one of the six planes. The maximum packed direction is <111> and its Lattice constant is a=0.332nm. [7]
Commercial pure Ti has a B transition temperature at 882°C. This temperature can change by alloying transformation from B to A phase. This is a thermo-mechanical process unavoidable. Titanium and its alloys are affected by this allotropic transformation: (β–>α ;β–> α +β ;β–>α +β–>α). Which has a huge influence over the physic and mechanical properties. [7]

1.4.1 Cooling process. Beta to Alpha transformation. Burgers relation.

When we cool the titanium from β phase, below the temperature transition, the maximum packed planes of β phase, BCC (100), are converted into basal planes (0001) of the α phase, HCP. Which produces an atomic distortion. The relation between the crystallography orientation of the α phases and β is called Burgers relationship:

$$(100)_\beta \parallel (0002)_\alpha$$

$$\langle 111\rangle_\beta \parallel \langle 1120\rangle_\alpha$$

According to this relation the titanium can generate until twelve different orientations of α Ti after the allotropic transformation. [7]

1.5 Alloying

1.5.1 Types of allowing elements in Ti

Titanium can be alloyed with thirty different elements by atomic replacement occupying interstitial spaces. This is possible thanks to the medium diameter size of titanium. [6]
As the figure 3 presents, there are three types of allowing elements in titanium: A Stabilizer (to raise the T_β_transition), the B Stabilizer (to lower the T_β_transition) and Neutral Additives (no effect in T_β_transition). Whithin the β Stabilizer we found the B-eutectoid stabilizers, where alloying element forms intermetallic precipitates (α+β–>α) and B-isomorphus stabilizer, where the additive forms a solid eutectoid system (β–>α+β).[6]

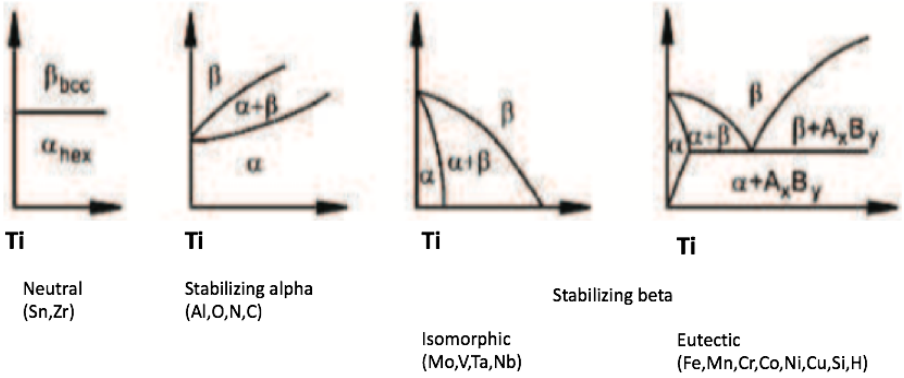

fig3. Phase Diagrams of titanium[9]

1.5.2 Classification Ti alloys

Titanium shows different possible alloys. A alloys are exclusively HCP phase, β alloys are BCC phase and α+β alloys present two versions. The first, alloys almost α consist of a small amount of βgen elements (weight 1-2%) at ambient temperature that present a similar behaviour to the α alloys. And the second, alloys almost β consist of a Small amount of αgen elements at ambient temperature that are similar to β alloys. [6][7]

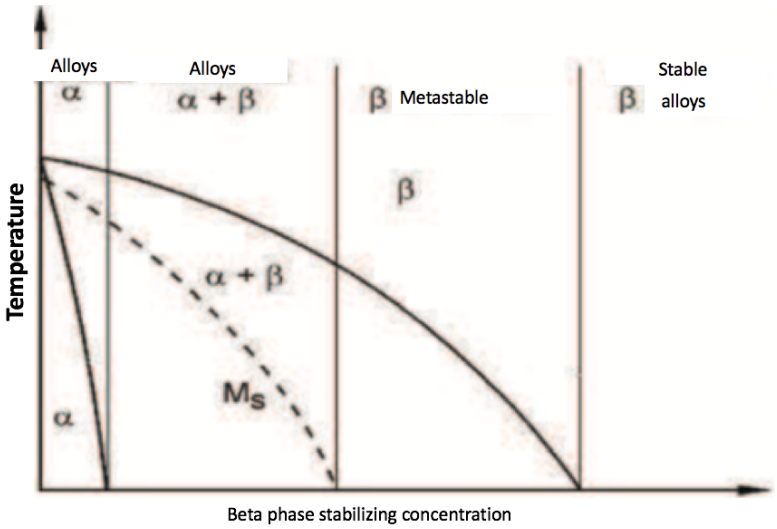

fig4.Relation kind of alloy with temperature and B phase stabilizing concentration [46]

A alloys have a good creep resistance and weldability, good corrosion resistance but they don´t admit thermal treatment.
B alloys retain β phase and they don´t suffer martensitic transformations after fast cooling. They have bigger βgent content than α+β alloys. They are metastable β alloys that can be used in multiples commercial applications. To get this type of microstructure we need apply over the material a treatment; solubilisation, temper and maturation to increase the resistance. We obtain the α particles disperses inside β phase retained. Other interesting properties are a high capacity to be strengthened, thermally treatable, good mechanic resistance and permit the welding process.
The α+β alloys present a range of 5-40% of β phase at ambient temperature. These alloys undergo martensitic transformation when they are cooled very fast. They present a perfect equilibrium between ductility and resistance, accept thermal treatments and aging processes. The α+β alloy most used is Ti-6Al-4V. [7]
However, in the market we can found Commercial alloys of pure Titanium (CP) under the international Norm ASTM. Pure titanium usually is weak; it loses its resistance at high temperatures but it has a high corrosion resistance. [6] It presents a low degree of pollutants concentration, except with the oxygen. The more dissolved oxygen appears in the alloy the higher resistance presents and the lower deformation capacity has. [10]

	Tensile strength	Yield strength	Concentration of pollutants (% weight)				
ASTM grade	Mpa	Mpa	N	C	H	Fe	O
1	240	170	0.03	0.08	0.015	0.20	0.18
2	340	280	0.03	0.08	0.015	0.30	0.25
3	450	380	0.05	0.08	0.015	0.30	0.35
4	550	480	0.05	0.08	0.015	0.50	0.40
7	340	280	0.03	0.08	0.015	0.30	0.25
11	240	170	0.03	0.08	0.015	0.20	0.18

Table2. mechanic parameters for different commercial alloys of pure titanium.[10]

Types	Titanium alloys
α	Ti-5Al-2.5Sn
α/β	Ti-8Al-1Mo-1V; Ti-6Al-2Sn-4Zr-2Mo, **Ti-6Al-4V**, Ti-6Al-6V-2Sn; Ti-3Al-2.5V; Ti-6Al-2Sn-4Zr-6Mo; Ti-5Al-2Sn-2Zr-4Cr-4Mo, Ti-10V-2Fe-3Al
β	Ti-13V-11Cr-3Al, Ti-15V-3Cr-3Al-3Sn, Ti-3Al-8V-6Cr-4mo-4Zr, Ti-8Mo-8V-2Fe-3Al, Ti-11.5Mo-6Zr-4.5Sn

Table 3. chemical composition in different types of titanium alloys[10]

1.6 Ti-6Al-4V alloy

The most widely used of all titanium alloys with many aerospace, industrial and medical applications. It occupies around 50% of global titanium production. It was developed in the 50th by technologic institution of Illinois, EEUU. The aerospace industry demands the 80% of the total production, while the rest is used in other areas like medicine, chemistry, automotive sector…
It is an α-β alloy that can be manufactured in all types of mill products. It is used in low to moderate-temperature applications limited to about 350ºC. It has good corrosion resistance a cause of its ability to form protective oxide layer, passivation principle. Although corrosion resistance is not as good as for pure titanium.[15]

Chemistry Limits	**UNE-7301 [%weight]**	**ISO 5832-3**	**ASTM F136**	**Physical Properties**	
Al	5,5-6,5	5,5-6,75	5,5-6,5	Density (lbs/in^3)	0,160
V	3,5-4,5	3,5-4,5	3,5-4,5	Elastic Modulus (x10^6 psi)	16,5
Fe	0,25	0,30	0,25	B transus T (ºF)	1830
C	0,08	0,08	0,08	Weldability	Fair
O	0,13	0,20	0,13		
N	0,05	0,05	0,05		
H	0,012	0,015	0,012		

Table 4. %weight composition according to different norms[15]

Mechanical Properties:

It is unique a cause of its exceptional properties of resistance, ductility, fatigue and tensile strength

			Pollutant limit (%max weight)				
Alloys α+β	σ_f	σ_{ys}	N	C	H	Fe	O
Ti-6Al-4V	900	830	0,05	0,10	0,0125	0,30	0,20

Table5. characterisation of Ti-6Al-4V alloy.[13]

Ti-6Al-4V is heat treatable and comes in both annealed and solution treated and aged (STA) conditions.

Mechanical Properties		
Guaranteed Minimum	Annealed condition	Solution Treated and aged (STA)
Ultimate Tensile Strength-ksi	130	150
Yield Strength -Ksi	120	140
Elongation %	10	10

Table 6. Most commons treatment in Ti-6Al-4V alloy. [13]

The higher the oxygen, nitrogen, aluminium or vanadium content the better resistance. The lower content the better tensile strength, ductility, corrosion resistance and lower crack propagation.
It is frequently used with a mill-annealed microstructure. Which presents a good relation between resistance, tenacity, ductility and fatigue. Of course considering different aspects like cooling process, thermal treatments and chemical compositions. Especially the oxygen concentration influence. [13].
In short, the ti6Al4V as α+β alloy can show different compositions of A, B phases. Depending of the thermal treatment used and the interstitial elements concentration in the alloy.

1.6.1 Cooling Ti6Al4V. Beta to Alpha transformation

When you realize a long-term cooling the B phase turns into α plaques, also known as Widmanstatten, which is characterized by its laminar structure. This structure presents improvements such as high tensile strength, high corrosion resistance, better fluency resistance and lower crack propagation. To improve more the properties sometimes is better to realize a re-crystallizing by annealing, which improves the ductility and the fatigue life. [12]
If the cooling is produced from a temperature higher than B Transus temperature (1830ºC), the transformation produces Alfa' (martensite). If the cooling is produced from a temperature lower than B Transus temperature, around 900-1000ºC, the transformation produces a mix between α phase (Widmanstatten lamellae) and A' phase (martensite). If the cooling rate is too high, we can find A'' phase in the final microstructure. Which is another type of martensite. It is characterized by its orthorhombic structure and its thermo elastic properties with shape memory. On the contrary, the microstructure A' is characterized by its hexagonal structure without shape memory capacity. As we can observe in the Fig5. The higher cooling rate, the thinner and longer lamellae microstructures. In summary, controlling morphology of the sample can be done through heat treatment and cooling rates. [12][13]

Cooling rate ($K\,s^{-1}$)	Phase composition Ti–6Al–4V
48	$\alpha'(\alpha'')$
40	$\alpha'(\alpha'')$
18	$\alpha'(\alpha'')$
9	$\alpha+\alpha'(\alpha'')$
7	$\alpha+\alpha'(\alpha'')$
3.5	$\alpha+\alpha'(\alpha'')_{trace}+\beta$
1.2	$\alpha+\beta$
0.08	$\alpha+\beta$
0.04	$\alpha+\beta$
0.024	$\alpha+\beta$
0.008	$\alpha+\beta$
0.004	$\alpha+\beta$

Increased cooling rate with finer shorter α-lamellae

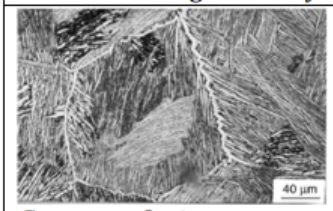

Common α-β microstructure exhibiting α-lamellae in a β-matrix

Decreased cooling with longer thicker α- lamellae

Fig 5. Influence of cooling rate on phase composition[12]

1.6.2 Metallography. Microstructures.

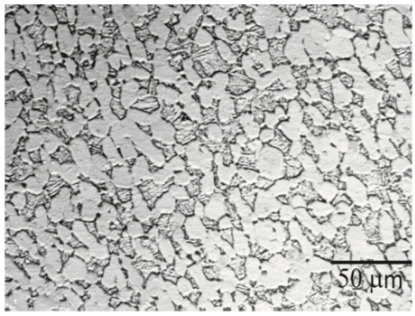

Fig 6. Ti6Al4V mill-annealed microstructure [12]

Fig 7. Ti6Al4V duplex microstructure[12]

The first type is equiaxiaxed microstructures. In the figure 6, Mill-annealed is produced when we work the alloy mechanically inside range of temperatures to get α+β. After we need agree an annealing process below martensitic temperature. This structure shows fine grains of α+β. Also within equiaxiaxed microstructures we found duplex microstructure Fig 7. If we augment the cooling rate after the annealing process, the β grains are transformed into α´´(fine lamellas), also called Transformed B.[12]

Fig 8. Ti6Al4V martensitic microstructure[12]

The second type is acicular martensite. Fig 8. We can get it by high cooling rate or by temper from a temperature higher than Transus temperature. In the titanium we can found two types of laminar microstructure. Massive (all the lamellas are in the same direction) and acicular. In the case of the Ti6Al4V, we can only obtain acicular disposition with similar lattice constant (a) of phase α. Depends of the cooling rate we can differentiate two types of martensitic structures: α' Phase, hexagonal martensite without thermic shape memory capacity and α" Phase, orthorhombic martensite with thermic shape memory capacity [12]

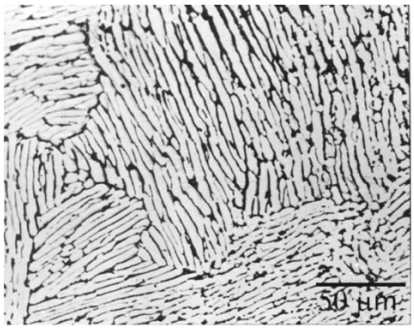

Fig 9. Ti6Al4V Widmanstätten[12]

The third type is Laminar or *Widmanstätten.* If we slowly decrease the temperature higher than Transus temperature until biphasic region α+β. α nucleation in grain β frontiers, growing in laminar way. As we will see in the SLS sample, this microstructure is characterized by Packets or colonies of α phase gross plaques and thin plaques of B.[12]

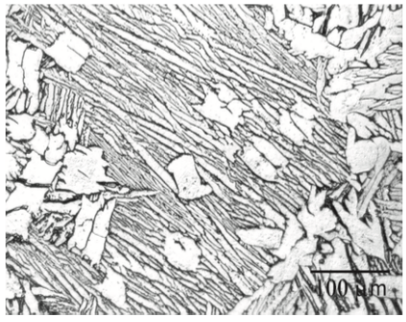

Fig 10. Ti6Al4V bimodal microstructure[12]

In the last case, Fig 10. Bimodal microstructure is identified by Isolated α grains respect to transformed β matrix (secondary α layer). It is produced by Annealing at 950ºC, temper with water and aging process at 600ºC. If it ages at 650ºC, the phase β grains are discomposed in phase α grains[12]

2. ADDITIVE MANUFACTURING

2.1 AM introduction

Additive Manufacturing (AM) system has been used from more than 50 years. In the beginning, it was used like a prototyped method but nowadays it plays an important paper as final piece production. The working premise consists of a feedstock material melted into near-net shape. The making is realized layer by layer until the final product is obtained. The piece is previously designed by computer software, CAD model. The sequence of manufacturing and the type or material are selected in the designed stage, so the CAD file must have all this information. At present, the researches develop the AM systems to improve their capacities and quality. The system is compatible with different types of metals and polymers. Furthermore, some systems are capable of use several materials at the same time. In metals case, until 2 metallic materials can be used in the same operation. In contrast with the traditional manufacturing process, AM is very useful to make prototyped pieces under request. We can get complex geometry pieces with different scales in a short space of time and in one step.

Depends heat sources	Feedstock material
Laser	Wire
	Powder feed (LMpD)
	Powder bed (SLS)
Electron Beam	Wire
	Powder bed
TIG arc	Wire

Table 7.AM methods more used in the aerospace industry [15]

2.2 AM Techniques for Ti-6Al-4V analysed in this research

2.2.1 SLS: Selective Laser Sintering sample

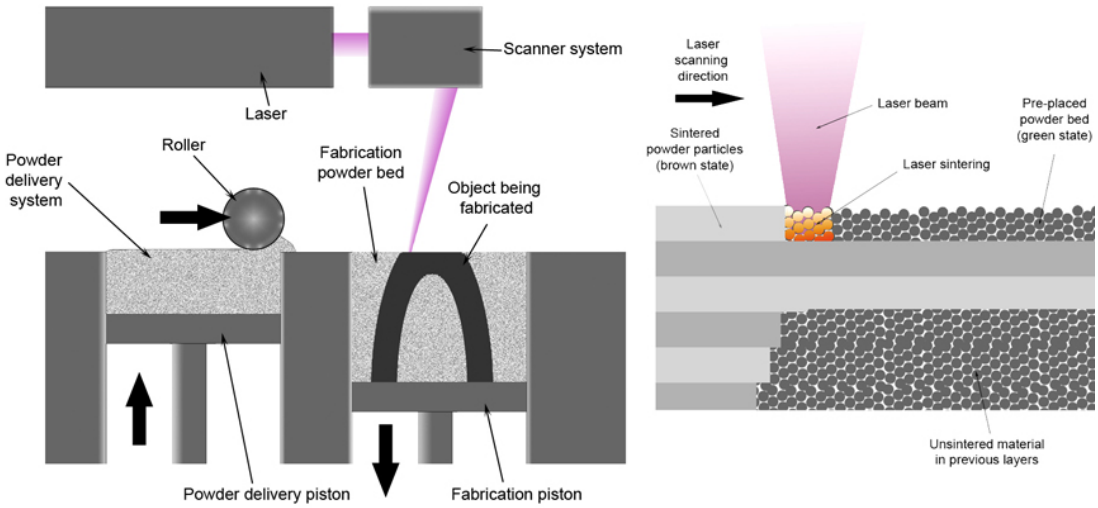

Fig 11. Selective Laser Sintering process(SLS) [16]

It is mainly used like rapid prototyping technic. It consists of depositing a thin powder layer on a piston surface previously heated at a temperature lower than powder fusion temperature. Then, a laser ray of high power (CO2) synthesises(fusion and solidification) the powder in the selected points. The piston descends and other layer of power is added repeating the process and building

the three-dimensional shape desired. It is a continuum process with huge flexibility. Which permits use a lot of different types of materials: polymers (nylon, polystyrene) or metals (steel, titanium, alloys….). In general, we will use this type of manufacturing with small pieces that require a good functionality. The dimensional information about the piece comes from a computer file previously designed. The quality of the density in the final piece depends more on the power laser than the process duration. It doesn´t need supports because the synthesised part is surrounded by powder all the time. It is possible use one metal powder component to build the piece. But in general the powder will have double component. You can choose between completely or partially molten metal or synthetized in liquid phase. Depending of the material and the laser used, we can reach the 100% in density of the material in the piece, with similar physic properties, close to use traditional methods. It is very useful with very complex geometry models. In the beginning it was used like prototyped system buy nowadays we can use it to create short production series of final pieces. [16]

2.2.2 LMpD: Laser Metal Powder Deposition

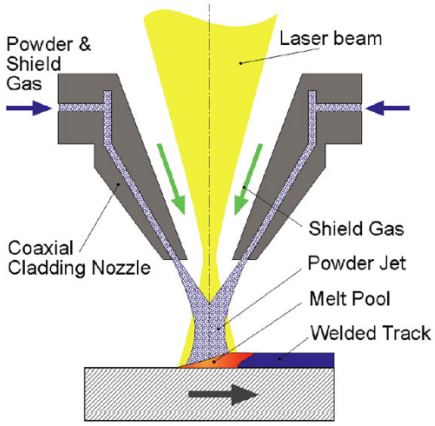

Fig 12. Laser Metal Powder Deposition (LMpD)[19]

Metal powder is injected directly into a laser beam focused of high frequency. Powder is melted and deposited over a base. The beam follows the marked trajectory creating the piece. It is not necessary do the process under controlled atmosphere (vacuum or inert gas). This method presents several advantages in contrast with other AM. It is very useful to repair complex pieces and tools because it is possible print directly over the metal piece to repair missing parts. It is very useful to repair and reconstruct moving mechanics pieces under wear effects. It can make pieces with different materials, so we can select what areas will have a specific material or other. LMpD is widely used to make big pieces thanks that it doesn´t require special conditions or deposit powder over big surfaces. However, by this method, we can´t obtain high precision because it is impossible to check what is the exact position where the melting powder will fall. So we always need to reprocess the piece. [17] [19]

2.3 AM Ti6Al4V characterization

2.3.1 Microstructures AM

The characteristic microstructure of AM with Ti6Al4V consists of large columnar prior β grains that grow in the temperature gradient direction. Depending on the AM process used, the size of the characteristic microstructure changes. This is a consequence of the cooling speed. Higher speed, then finer microstructure with hardness increased. In general, the common microstructure is formed by the prior β grains that contain inside α laths separated by retained β, Widmanstätten structure. The α structure presents two possible forms, colony α or basketweave α micro-structure. [20]

The parallel bands appear with AM processes using wire or powder (LMpD) as feedstock material but not with powder bed (SLS) [17]. They are visible along all the structure excepts in the extremes of the sample. They are not related with the layer deposition. The parallel bands are formed by α colonies, while in the spaces between the band we found basketweave α. The cause of the parallel bands formation is the contact between a cold layer previously placed with the next layer heated. This produces a thermal gradient that causes the reheating of the previous layer. If the temperature of reheating is around the transus temperature, we obtain this kind of structures a cause of the rapid cooling. This is known because this structures are not affected by thermal treatments below β transus temperature. The direction, where is the highest temperature gradient, defines the solidification direction. It is established in <100>. This explains why the columnar β grains cross several layers of deposited material. On the other hand, The crystallography orientation of the grain boundary (α) is established from the Burgers with the adjacent prior β grain. The α colonies, inside of the same prior β, grow on both sides of the grain boundary. [15]

2.3.2 Mechanical properties

The Ti-6Al-4V material shows a clear anisotropy in the mechanical properties. As we can see in the table 8[15], there are important changes in tensile properties according the deposition direction, parallel or perpendicular.

Heat source	Feedstock material	orientation	yield strength [MPa]	Breaking load [MPa]	Elongation [%]
Cast			896	1000	8
Wrought, annealed			925	1000	16
Laser	Powder feed (LMpD)	Parallel perpendicular	1066 832	1112 832	5.5 0.8
	Powder bed (SLS)	Parallel perpendicular	1195 1143	1269 1219	5 4.9

Table 8. Tensile properties of AM Ti-6Al-4V samples used in this research (700-730ºC 2 hours)

It's important to compare the tensile properties from the conventional production methods in the metallic alloys, as Cast or wrought with annealed, respect to the procedures used to get the samples analyzed in this report. As we can see, the values are below in the conventional methods and the elongation is better in the perpendicular deposition direction [18]. However, the parallel deposition shows better tensile properties, as yield strength or breaking load, than the other case. Although the table doesn´t show it, the powder-based methods have better tensile properties than the wire-based methods. Especially, if the source of heat is the laser. The powder-based processes exhibit finer microstructure than the wire-based AM processes, because of the less heat input during manufacturing and thus higher cooling rate. [17]
As we will see in the data analysis, the sample from SLS AM showed better behavior with the electro-polishing, permitting the etching too. This is explained by the physic properties shows in the Table 8 consequence of the reheated until Transus temperature that the melted powders suffer when they are cooled in contact with the other heat powder in the melt pool. It happens the contraire with the LMpD sample from parallel deposition direction. It shows disperse areas with martensitic structure along its surface. Which gives good properties of hardness and mechanic resistance but lower than the reheated effect suffered by SLS microstructures. A slightly higher fatigue life is reported for the parallel orientation respect to perpendicular orientation deposited layers
The literature doesn't mention enough information about the crack initiation. But the experience shows that it appears in the manufacturing AM defects. Such as slip, locations accompanying inclusions, pores or weak points in the microstructure. It is worth mentioning that the cyclic charges in the fatigue origins diverse defects too.[15]

2.3.3 Debilitating effects of AM

There are two types of defects frequently observed, pores and lack of fusion. The Mechanical pore formation is happened because of the contamination by water, gas created during addition process, air, waste material. On the other hand, metallurgical pore formation is generated by oxygen, hydrogen and nitrogen in the melt pool. Other debilitating effect is Lack of fusion. It happens when the previously layer is not completely remelted. This is caused because a large melt pool tends to flow in front of the heat source, covering and preventing the previous layer to be completely melted. Possible causes of this are a heat input too slow, too high welding speed, incorrect position of the heat source, incorrect position of the wire feeder, mistakes in parameters selection creating instability in the melt pool. This defects have an important impact on the mechanical properties. Specially in the fatigue. When we have a big pore size or its position is close to the surface, the behavior against fatigue decreases [21].
In the system based in wire feedstock appears higher residual stresses in the deposit parallel direction than the perpendicular. With regard to the system based in powder feed, when the subtract or the previous layer is preheated, the residual stresses decrease. This is explained by the fact that in an ambient at high temperature the cooling is lower than with less temperature. So less temperature gradient and less residual stresses. [21]

3. ELECTROPOLISHING

3.1 Process

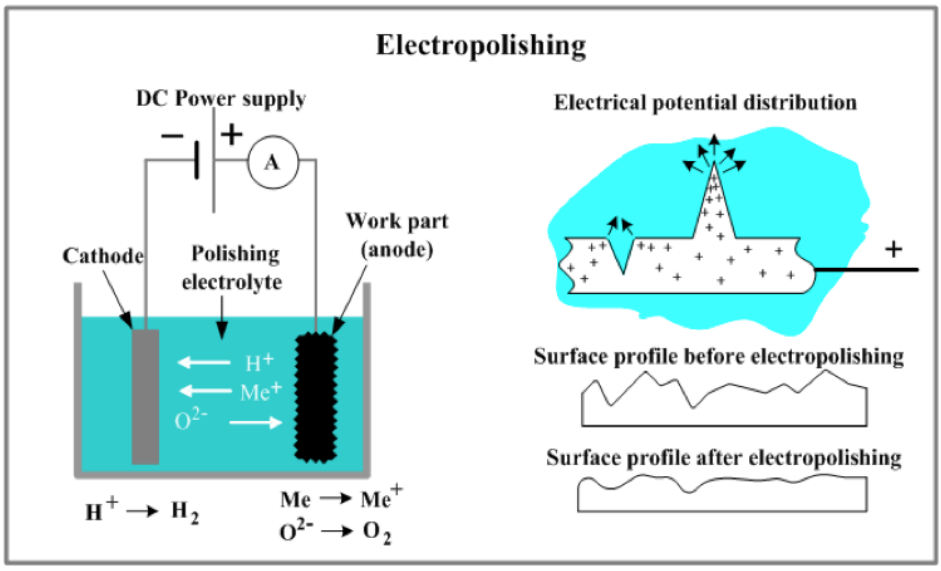

fig 13. Electro-polishing technique[22]

Superficial treatment where the polished metal acts like an anode, which loses its electrons, into an electrolytic cell. To get it, we apply current that makes a polarized film over its surface. Which permits the metallic ions diffusion. The thickness of the layer is not constant. It is bigger in the valleys (high resistance) and lower in the peaks. The areas with burrs have more current density too. So that, they are dissolved faster than the rest. With this process we can get a flat surface with high brightness. To do this process we have different control parameters. It is important to know which are their effects to get the best polished quality. Area treated, electrolyte, exposition time, temperature, flow rate, voltage (or current intensity). [22]
The goals of an ideal polishing are smoothing, low microscopic irregularities (>1μm) eliminating peaks and valleys, and polishing, removing small irregularities (<1μm)

The thickness of the dissolved material varies from 10 to 25 μm, in function of the voltage used and the exposition time. So usually we need to use the manual polishing before until get at least

a medium quality. By electro-polishing we can improve several surface aspects such as surface levelling, remove scratches and micro-holes elimination. Which avoids the accommodation of strange elements, eliminating the risk of the beginning of localized corrosion processes. [23]

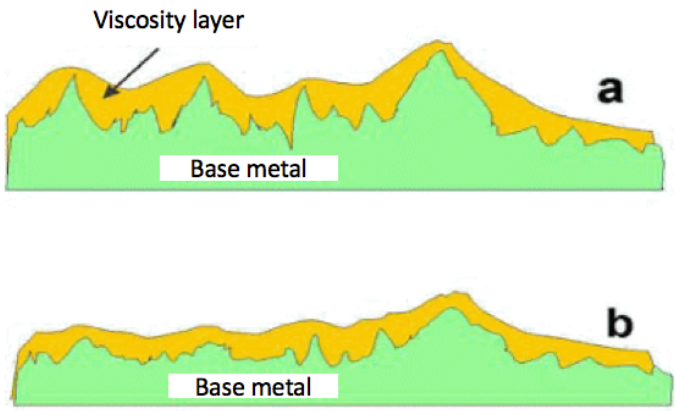

Fig 14. Polishing layer actuation.

a. In the beginning
b. *Before electro-poslishing [23]*

The surface obtained with the electro-polishing process is different from the mechanical polishing. The final objective is to get the mirror surface. To get it, we press the sample on papers with different roughness and particles harder than the treated material. Normally we work with SiC papers or diamond particles dissolved in special liquids. Observations at a microscopic scale shows that is better eliminate the micro-holes where strange imperfections can be accommodated because of localized corrosion). So as we will explain not always the mirror surface is the best option [24]. To get the perfect polishing surface the metal must show a homogeneous surface, free from superficial defects. The defects occulted by mechanical polishing are revealed by electro-polishing. It is the opposite process to galvanised. Whereby the metallic ions are in the solution and they are deposited over the sample surface. [23]

3.2 Advantages. Comparison with Mechanical polishing.

Electro-polishing is recommended to treat pieces with irregular shapes or with big size. We can get results very fast and reduce the labour for the operators. It descends execution times and costs a cause of automatic process. It increases the corrosion resistance because it leaves a passivating layer over the metal surface. This is produced a cause of the oxidant environment around the surface treated. It decreases the adhesion of liquids and solids. So it improves the cleaning. It can polish pieces with a complicate geometry getting uniform surfaces with only one step.
Really, by mechanical polishing we can obtain a smooth surface where the light only reflects in one direction. The surface obtained usually presents deformations and superficial damages. Furthermore, by electro-polishing we can get a surface free of scratches and tensions. Which presents a three-dimensional structure reflecting the light in all directions. We obtain a glossy aspect respect to mirror surface in mechanical polishing. [25]

3.3 Influential Parameters in polished quality

In general, the quantity of material eliminated depends of the voltage applied, the exposition time and the efficiency of the electrolyte.
The size of the grain has influence in the final polishing quality. A structure with small grain shows better final surfaces than the structures with big grain where the final surface is irregular.

Depend of the voltage applied, the current intensity and the application area we can obtain different results of polishing. It depends of the material to treat and the field of use

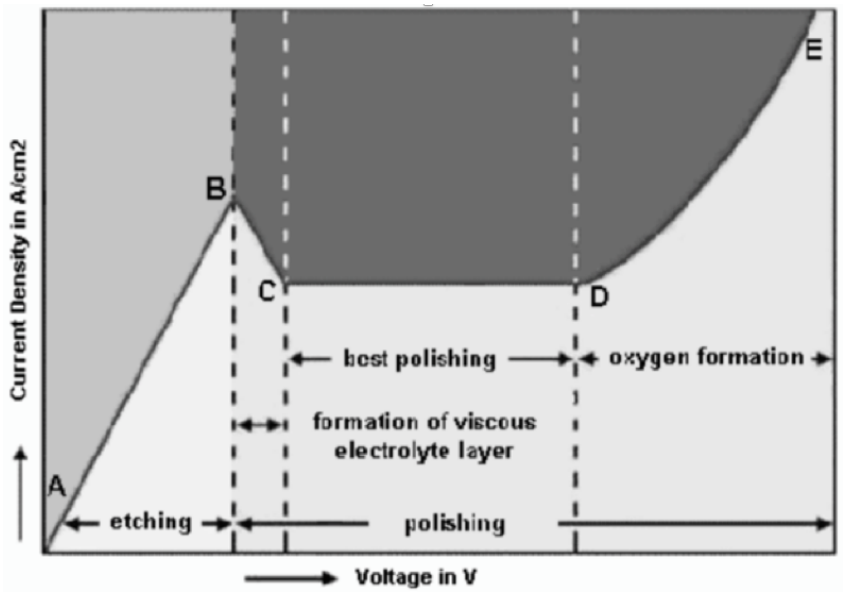

Fig 15. Curves of current density vs voltage during electro-polishing [24]

We can differentiate 3 operative regions:

- A-B Etching zone. We use it to define the grain frontiers. (very important to analyse and identify the microstructures by SEM and EBSD)
- B-C Formation of electrolytic viscous layer. The resistance augments so the current density descends.
- C-D Range with the best polishing. In our case (19-21V)
- D-E We can obtain polishing but the excess in gas formation on the sample surface origins defects and scratches. Which descends the final quality of the sample and difficult the microstructures identification by SEM and EBSD

At low voltage, electro polishing is only effective in areas close the edges of sample. But at higher voltages, the oxide cover is detached from the Ti surface. Which was exposed to electrolyte, alternate formation and detachment, causing many pits and cracks.

The electro-polishing time is an important parameter. As we will see in the experimental part of this report, with short times the electrolyte can't remove the oxide layer, that protects the titanium surface, and the polishing is almost ineffective. With an adequate amount of time, the formation and detachment of oxide layer is happened. Which implies a final smooth surface. Electro polishing for longer durations, would lead to several pits and cracks formed on the surface a cause of the micro-roughness effect.

In general, if the temperature is higher, the electro-polishing works faster. With the temperature the particles diffusion is more active so the treated area loses more metallic cations. At the same time the oxidation process accelerates the passive layer formation.

The bigger treated area, the longer application time. Remember that one time the area has reached the polished surface, if we continue with the process, there is a risk of generate micro-roughness.

Depending of the acidity or aggressiveness of the electrolyte the effect over the sample will be different. So we would have to adjust the parameters, time or voltage.

It is important check the electrolyte state too. Each certain number of uses we need to change it, because it loses its polish ability.

One time we have finished, it's important clean the sample and the equipment to eliminate the rests of electrolyte. Which is very aggressive. Especially, we must to take care with the cathode because it can contain rest of electrolyte or cations joined.

At low stirring speeds, the current density decreases due to formation of oxide layer which is not being separated from the surface. Thus obtaining unsmooth and cracked surface. Low agitation speed does not supply enough physical force to remove the layer from the surface.

At increased agitation speed, the anodic current density increases from the beginning. The final surface is smooth. But further increasing of the agitation makes the surface matt and less smooth. The concentration polarisation can be primarily reduced at high stirring speeds, corrosion rate was increased and electric field distributed non-uniformly on the surface due to formation of bubbles on the surface, thus leading to corrosion [26]

4. SEM AND EBSD

4.1 SEM: Scanning Electron Microscopy

Scanning Electron Microscopy (SEM) is a technique where an electron beam under vacuum conditions is focused onto a solid sample surface. The electrons from the beam interacts with electrons in the sample, generating different types of signal that can be detected and provide information about sample surface topography and chemical composition of the sample. The magnification that can be achieved in a Scanning Electron Microscope depends on how narrow the beam of electrons that strikes the surface can be, and can reach 1 nanometre, about the size of 3 to 5 atoms. The control of the beam is achieved using magnetic fields, with other magnetic fields being used to shape the beam, and to move it across the sample. The range of magnification may range from 30x to as high as 500,000x [28]. Samples can be observed in low vacuum which avoids interactions with the beam during the acceleration. In wet conditions and at a wide range of cryogenic or elevated temperatures.
The most common SEM mode is detection of secondary electrons emitted by atoms excited by the electron beam.

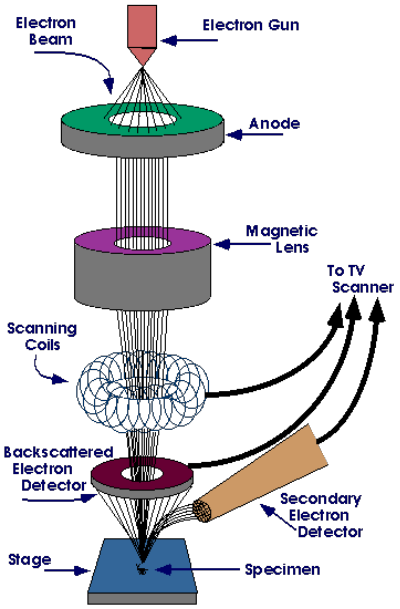

Fig 16. The action of the electron beam stimulates emission of high-energy backscattered electrons and low-energy secondary electrons from the surface of the specimen. [27]

OPERATION PROCESS:

1. The electron gun, located at the top or bottom of the structure, fire a beam of electrons (primary electrons) at the sample that we are analysing. We use an electric champ E to accelerate the electrons that exit from the electron gun. Depend of the power E we can use the SEM to analyse biologic specimens (E created with low voltage 50V) and metallic samples which don´t suffer damages with high voltages 30000 V, so we can obtain better resolutions

2. The magnetic lenses have used to focus electron beams to get clear and detailed images from the sample. They are made of magnets that permits change the path of electrons fired from the electron gun
3. One coil permits give the correct orientation to the electrons beam. We can change this orientation to scan all the sample surface.
4. The sample is put on the stage inside the sample chamber. Due to the sensitive of SEM, we must fit the sample and avoid vibration during the process
5.The thin beam of electrons impact in a small area of sample surface. Which produces an interaction between sample atoms and electrons of beam.
We can found different possibilities: Beam electrons bounce off of sample surface, beam electrons conducted away and beam electrons transmit energy to sample electrons of area scanned. This implies the appearance of ray X that the detector catches and transforms in a picture that we can see. Secondary electron images show morphology and topography of the sample. The more the number of electrons reaching the detector, the brighter the image is. On the other hand, secondary electrons are produced by inelastic interaction of beam electrons with interaction, there is energy loss. Backscattered electron images show difference in atomic number over a sample. The higher the atomic numbers of the atom, the more backscattered are bounded back, making the image brighter for larger atoms. Other aspect is back scattered electrons are produced by the elastic interaction of the beam electron with nuclei of atoms in the specimen.
The electron beam is affected by air and water molecules, so the sample must be placed in a vacuum chamber. The sample must also be conductive to allow the electrons not reflected or absorbed to be conducted away. This is done in order to preserve the sample and keep it from changing or decaying throughout the scanning process.
Before using the SEM, we must assure that the sample is clean, dry and shows a good electrical conductivity. If the sample doesn´t conduit the electricity we can cover it with conductive material as golden, silver, copper… Furthermore, the system permits to analyse organic and inorganic solid samples.
Assure an optimal polished surface in the sample is very important to get the signals abovementioned in the right way. It´s for that in this report we have analysed the best way to get a correct polishing. It's very important to place the sample with the correct orientation too. For that we have different tools as silver liquid or sample holder. [29]
The SEM can be equipped with different detectors, including the following: SEI (Secondary Electron Image) is a secondary electrons detector that generates high resolution pictures, BEI (Backscattered Electron Image) is a detector of retrodispersed secondary electrons that permits to obtain pictures with the composition and the topography of the sample surface and EDS (Energy Dispersive Spectrometer) is a detector of X-rays, generated from the sample, that permits to realize several analysis and images of elements distribution in polished surfaces [30]

4.2 EBSD: Electron Backscatter diffraction

EBSD (Electron backscatter diffraction) is a microstructural-crystallographic characterisation technique to study any crystalline or polycrystalline material. The technique involves understanding the structure, crystal orientation and phase of materials in the Scanning Electron Microscope (SEM). Normally we use EBSD to explore microstructures, revealing texture, defects, grain morphology and deformation. Experimentally EBSD is conducted using a SEM equipped with an EBSD detector containing at least a phosphor screen, compact lens and low light CCD camera. [31] The biggest advantage of the high-resolution detectors is their higher sensitivity and therefore the information within each diffraction pattern can be analysed in more detail. Modern EBSD systems can index patterns at up to 1800 patterns / second. This enables very rapid and rich microstructural maps to be generated.

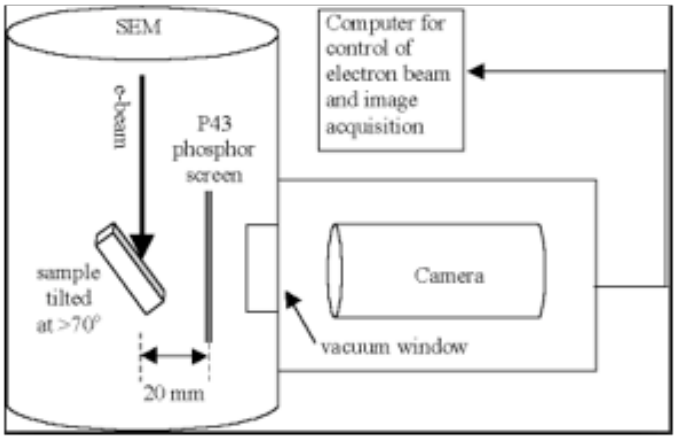

Fig 17. EBSD process scheme[31]

The phosphor screen is located within the specimen chamber of the SEM at an angle off approximately 90° to the pole piece and is coupled to a compact lens which focuses the image from the phosphor screen onto the CCD camera. [31]

EBSD PROCEDURE:
1. A polished crystalline specimen is placed in the SEM chamber at a highly tilted (70º from horizontal) towards the diffraction camera.
2. The beam of electrons hits the sample. Some electrons are diffracted (other are absorbed by the sample) and can escape the material and some will collide and excite the phosphor causing it to fluoresce.
3. Escaping electrons may exit near to the Bragg angle and diffract to form Kikuchi bands which correspond to each of the lattice diffracting crystal planes. In most materials, only three bands/planes which intercept are required to describe a unique solution to the crystal orientation. This crystal orientation relates the orientation of each sampled point to a reference crystal orientation. This geometric description is related to the kinematic solution that gives the orientation and texture analysis but ignores many physical processes.
4. To adequately describe finer features within the electron beam scattering pattern (EBSP), we must use several dynamical model. After pattern collection arrive the process of indexing. This allows for identification of the crystal orientation at the single volume of the sample. With EBSD software, pattern bands are typically detected via a mathematical routine using a modified Hough transform. Angles between bands represent angles between lattice planes. When the angles between three bands are known an orientation solution can be determined [30, 31]
There are two methods of indexing: Triplet voting, whereby the program identifies multiple triplets (three planes) from the bands and gives votes of quality to know which is the correct triplet and minimising the fit between experimental and computer pattern, whereby the program considers all triplets possible and it compares with the bands.
In resume, the pattern of Kikuchi lines on the phosphor screen is electronically digitized and processed to recognize the individual Kikuchi lines. These data are used to identify the phase, to index the pattern, and to determine the orientation of the crystal from which the pattern was generated.

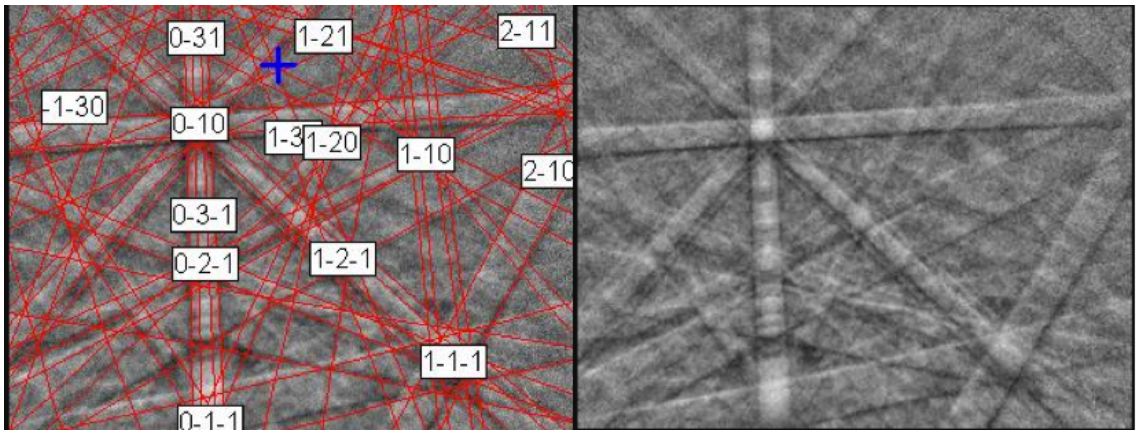

Fig 18. Kikuchi Bands identification by Software from SEM micrograph captured [31]

Pattern centre relates the orientation of a Crystal. It describes the distance of the interaction volume to the detector and the location of the nearest point between the phosphor and the sample on the phosphor screen. The most commercial EBSD systems utilize the indexing algorithm combined with an iterative movement of both crystal orientation and suggested pattern Centre location [32]

By scanning the electron beam, in a prescribed fashion, (typically in a square or hexagonal grid) results in many rich microstructural maps. These maps can spatially describe the crystal orientation of the material and can be used to examine: grain orientation, grain boundary, diffraction pattern (image) quality, grain size, crystallographic texture, the prior texture of parent phases at elevated temperature, the storage and residual deformation after mechanical testing and the population of various microstructural features, including precipitates and grain boundary character[32]

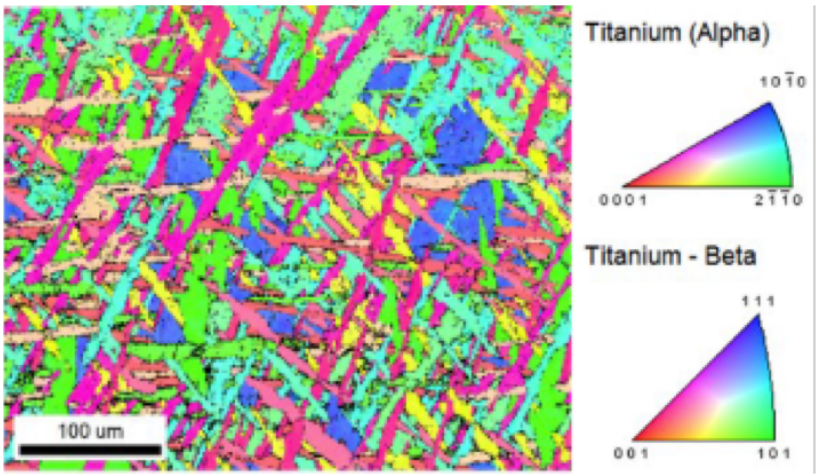

Fig 19. Electron backscatter diffraction (EBSD) pole figure map of the investigated Ti-6Al-4V: heat-treated prior to the caliber-rolling[33]

These maps are codified in colours using IPF (inverse polo figures) that helps the interpretation. To get the orientation of the microstructures we use an axe as reference and from it, we stablish the normal vector of the crystalline diffraction plane for each point. The technic permits study the α colonies structure with different scales. From them it can rebuilds the β primary grain structure. This is realized by a code that searches the common β prior grain of which the α microstructures are originated. The code works applying the Burgers relation in each point of the SEM image captured and then choosing the most probably B structure. This structure will be between the six possible orientations of the α crystal developed from original B grain. [33]

To get the best analysis possible by EBSD, we must considerer some aspects. EBSD works fine when we put the sample with an angle of 70º respect to the electron beam inside the SEM. This angle is necessary to permit the scape of the backscattered electrons from the polished surface of the sample verifying the BRAGG, rule about the interplanar space in the crystalline structure.
The method is very sensible (5nm), which is affected by small defects over the surface that block the signal and the correct microstructural identification. The mechanic polishing, even with master polishing (colloidal silica) doesn´t permit obtain any result by EBSD. If we use SiC papers, the polishing is too thick and the surface presents too scratches and irregularities. On the other hand, if we use a thinnest polishing by colloidal silica, we can eliminate some scratches and irregularities until get the mirror surface. However, this process creates an important structure deformation over the surface that blocks the signal. Even so, it is usual prepare the sample with mechanical polishing before use other complementary methods which only permit to eliminate a little amount of material. One time the mechanic polishing is done, we must use other polishing methods such as: Chemical polishing with abrasives, Polishing by vibration, Electro-polishing. (Method used in our research)[30]
Other important aspect is that we must use samples from materials with electrical conductivity. In the case contraire we must cover them with a conductive coat as golden, silver or copper.
The best solution is to use a stationary beam (scanning mode off) and acquire data over the area of interest by moving the sample. The procedure requires an automated specimen stage, and data acquisition is considerably slower than acquisition using beam scanning [34]

5. EXPERIMENTAL PROCEDURE

To develop this research, we have used two samples of Ti-6Al-4V made by different methods of additive manufacturing: Selective Laser Sintering(SLS), method based in powder-bed using laser, and Laser Metal Powder Deposition, method based in powder feedstock using laser.
In the first part, we have analysed the mechanical polishing with master quality, using colloidal silica, to compare the final surface respect to the polish area from electro-polishing. We have identified the best method to obtain the best results by EBSD analysis. To realize this part we have use the sample LMpD. In the second part we have evaluated the changes of the polishing quality with the variation of electro-polishing time. To develop this step we have used the SLS sample. In the third part we have evaluated the changes of the polishing quality with the voltage variation. In the fourth part we have set the optimal parameters to get the best polishing quality to use the EBSD. How we will see in the results, the parameters of time and voltage with polishing and etching of the SLS and LMpd samples have been different. Although the material used in both samples was the same, they have been made by different AM methods, with different cooling rate. So the have showed different microstructures with different properties. To set the optimal parameters of voltage and time for each sample. After each electro-polishing we checked the sample surface to know the polishing quality. If we obtained the optimal polishing, we analysed the sample by EBSD. If not, we repeated the polishing process. [35]
The EBSD is a very sensitive method that needs a perfect surface, flat and without scratches, to identify the microstructures that appear over the polished area. Any superficial damage can affect the results. When we talk about the concept of mirror surface, it means a surface without defects such as roughness surface, different polishing planes or scratches. To analyse a sample by EBSs is necessary reach this polishing degree.
One time we have prepared the samples, we use the electron microscope SEM and the EBSD (electron backscatter diffraction detector) to analyse it.

5.1 Preparation Samples. Grinding and electro-polishing

CUTTING
The first step is cut the sample.
SLS: cut perpendicular to the deposition direction.
LMpD: cut perpendicular to the deposition direction

I have chosen the face where we can found the microstructures growing in the deposition direction. This permits obtain better identification result from EBSD analysis.

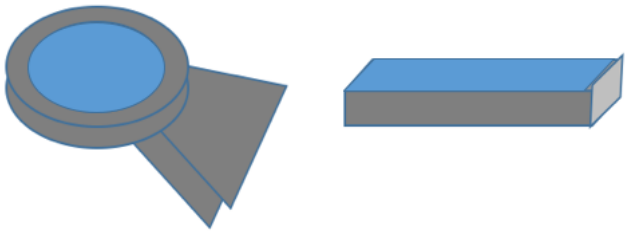

Fig 20. Polished surface section.

SEMIAUTOMATIC GRINDING

Before the electro-polishing we must do a mechanical polishing to remove material at macroscopic level. The procedure in both cases was the same, polishing with grinding papers with different accuracies (SiC paper of 1200, 2000 and 4000) by Metaserv 250 grinding semiautomatic machine. In the first experience we have compared the behaviour of the LMpD sample treated with master manual polishing and electro-polishing with the optimal parameters.
The master polishing is reached when after apply the SiC papers, we polish the sample by colloidal Silica (SiO_2). It is important to verifier that the sample doesn´t show scratches or surface roughness by optic microscopy. One time we have finished with the grinding; we clean the sample with water.

Fig 21. Equipment of mechanic grinding

To realize the best mechanical polishing, we must assure that the polished face is parallel respect to the SiC paper and we don´t apply too pressure. Thereby avoiding different planes over the surface which give us different focus areas during SEM analysis. After each polishing stage we must verifier the flat surface, the direction of the polishing scratches, and polish in the perpendicular direction in the next step.
We didn´t mount the samples because we didn´t found an electric conductive mounting to get the best electro-polishing area.
Due to the small LMpD-sample size, it was very difficult works with the mechanical polishing and get accuracy results. [35]

ELECTROLYTICAL POLISHING

One time we obtain a good quality surface. We prepare the sample by electro-polishing machine. In the Fig 22 we can see the machine used for this research. The Lectropol-5 of Struers. To use this machine, we must put the electrolyte recipient into the machine. Then select a plastic plate with the size of the polished area and on it place the sample in contact with the metal cathode.

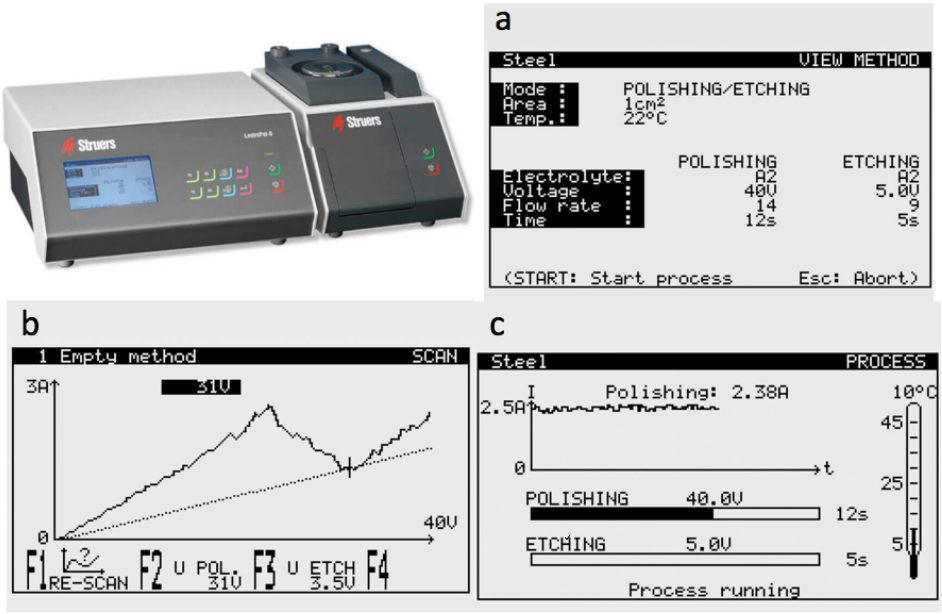

Fig 22. Equipment electro-polishing. [37]

In the Fig22.a we can see the control parameters to get the best polished surface. Depend of the sample is better use or not etching. And polishing with more or less time. Actually, in this project we have played only with the variation of time and voltage to improve the polishing quality.
The area used in both cases were 0.5 cm^2 a cause of the sample size. The room temperature was 22ºC. The electrolyte used with our material was Struers A3 and the flow rate 16, following the recommendation from data base (Struers) for titanium pure.[37]
The electrolyte A3 was created in the laboratory using the chemical composition found it in the maker website. [36]

600 ml	methanol
360 ml	butoxyethanol
60 ml	Perchloric acid

With each polishing the electrolyte absorbs more metallic cations until the moment where its efficiency decrease, it appears with yellow colour. At this moment we must change it.
In resume, we have use the following parameters to do each analysis. Only changing the time and voltage parameters.

Mode	POLISHING/ETCHING
Area	0,5 cm^2
Temp	22°C
Electrolyte	A3
Flow rate	16
Voltage	Variable
time	variable

To set the optimal voltage to get the best polishing possible, the machine has a scanner that gives us this value for our sample. We can obtain the optimal voltage from the polarisation curve Fig

22.b. Although we have used the same material with both samples, we will see how the recommended voltages were very different for each one.
The fig 22.b represents the polarization curve or density current versus voltage. In this representation we can differentiate three stages.

Stage1: The current starts to increase

During electro-polishing, cations leave the specimen surface and diffuse into the electrolyte, and current density increases with increasing the applied voltage

$Ti \rightarrow Ti+2 +2 e-$

Stage2: The current is almost stable

Constant current density with increasing voltage. When the anodic film is formed according to the reaction. This represents passive behaviour

$Ti+4OH- \rightarrow TiO2 + 2H2O+4e-$

Stage3: The current increases again

Current density further increases at higher voltages and the evolution of oxygen (O2) takes place on the Ti surface. Also known as the transpassive behaviour

As a result of high current density, pitting of the Ti surface may take place in this region

The fig 22.c represents the current density versus time curve. Current transients recorded during electro-polishing with a fix voltage. The drastic drop observed at the beginning of the current transient could be due to a passive insulating oxide layer formed on the titanium surface. Eventually, the physical bond between the oxide layer and the Ti surface is weakened due to the effect of methanol on the instability of the oxide film
Therefore, further anodic reaction will bring other effective means into action such as viscous force and turbulence which helps to separate the passive oxide layer from the surface
Once this takes place, fresh surface of Ti is exposed to the electrolyte and the anodic current approaches a constant magnitude corresponding to the rate of dissolution
In the second part of this research, we have analysed the effect of polishing and voltage time with the quality of final surface. This stage has realized using the SLS sample.
In each polishing, we have set an etching with 14V and 3s, voltage obtained from the polarization curve. In our research, the etching has played an important role as a post-process method by which improves the polishing accuracy. In general, with its application we have obtained better results with EBSD analysis. However, sometimes it is better don´t use it how in the LMpd case.
To know how the polishing time affects the surface quality in the polished area, we set a constant value of voltage (20V, obtained from polarisation curve) and by optical microscope we analyse differences over the surface with different times (unpolished,5,9,18,25 and 60 seconds)
To know how the polishing voltage changes the surface quality in the polished area, we set a constant time (25s, the best time of the previous analysis) and by optical microscope we analyse differences over the surface changing the voltage (unpolished,5,20 and 45V).
In the third part we have set the optimal parameters of time and voltage with polishing and etching to get the best EBSD results. Actually, the values of voltage have obtained from the polarization curve so we only have played with the time to reach the best polished area possible. In this case we have used the SLS and LMpD samples for ours experiments.
As stated above, we consider a quality polishing when the surface doesn´t show scratches, roughness and is flat, without polishing faces.
One time we have realized the complete polishing. We must clean the sample with ethanol to remove the corrosive electrolyte and the wastes. Then dry the sample with a dryer to avoid marks. After finishing with the electro-polishing machine is very important follow the cleaning instructions (clean with water and ethanol) to save the equipment in good condition.[38]

5.2 Analyse sample surface by optical microscope

We have used an optical microscope like a fast way to evaluate the surface quality of the sample. With the SEM the assembly process is more complicate. We have used the Microeclipse MA200 of Nikon microscope.

One time you put the sample under the microscope, you must focus the view and localize the polished areas. If the quality is enough we can go to the next step (SEM analysis), if not we must repeat the polishing process changing the control parameters.(V,t)

5.3 Analyse sample by SEM, EBSD, EDS

One time we have the optimal polished surface, we analyse the sample by SEM.
We mount the sample on a support in a manner that the polished area forms an angle of 70º with the horizontal platform. To join the sample with the support, we can use small screws or silver liquid. But it's very important assure the electrical conductivity during the analysis.
We put the sample mounted in the support inside of the vacuum chamber. We must put the sample with the correct orientation to assure the diffraction of the electrons from the electron beam, as we saw in the theory part.
With the SEM we search in the polished surface the area that shows the best quality. We focus this area and we assure the best signal reception for the EBSD and EDS receptors. With the EBSD we will obtain the phases proportion and their orientation and with the EDS we will obtain the chemical composition.

6. RESULTS DISCUSSION

6.1 Evaluation of mechanical polishing quality

In the first part of this research we have analysed the behaviour of the manual polishing with the EBSD analysis. To realize that, we have prepared the LMpD sample with the grinding papers from an accuracy of 1200 until 4000, then we have applied a master polishing using colloidal silica during several minutes. By this preparation we have obtained a polished surface how we can see in the Fig 22a.
When we have tried to analyse the LMpd sample with master mechanical polishing by EBSD. We haven´t obtained any results. This is explained by different reasons such as. When we use mechanical polishing we obtain a deformation area close to the treated surface. This area shows different properties in contrast with the base metal. This deformation is created by fluency, this mean that under the strong mechanic action by manual polishing, the material from the peaks is replaced filling the valleys. This superficial surface is called the Bieldy layer and it has several micrometres of thickness. The final surface structure is almost amorphous with oxide inclusions and waste of polishing material.
So that, the physical and chemical properties from a mechanical polished surface are different respect to the base metal. That origins mechanic stresses which could be the beginning in a corrosive process.[39]
On the other hand, when we polish a sample by manual polishing we only get one plane over the surface. So the electron beam is diffracted only in one direction. With the electro-polishing, the polished surface conserves the properties of the base metal. Furthermore, each microstructure is orientated in one direction so when the electron beam hit the sample it is diffracted in several directions. For this reasons we can obtain good results by EBSD.

a b

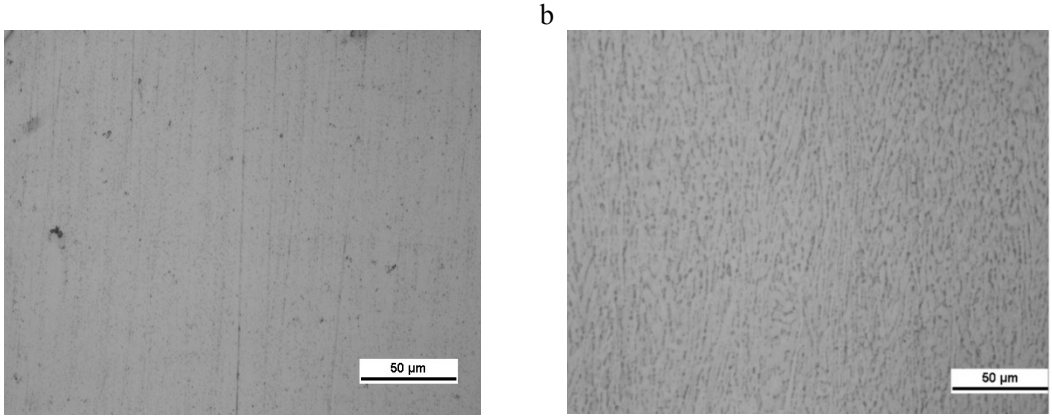

Fig 23. a/LMpD surface polished by paper of SiC and colloidal silica.(Master polishing)
b/LMpD surface polished by electro-polishing with optimal parameters of (t,V)

Since that time, we have decided use the mechanical polishing in combination with electro-polishing. It means use the different SiC papers to remove a huge amount of material and apply a final polishing by the electrolyte to improve the accuracy.

6.2 Variations of voltage and time in electro-polishing

SUMMARY OF EXPERIMENTAL PROCEDURE

Take the polished surface and analyse by optic microscope (Microeclipse MA200,Nikon). Repeat the processes with different polishing from changes in the voltage and time parameters. We have used the SLS sample with perpendicular cut. Material Ti6-Al-4V
Control parameters for the electro-polishing machine (Struers Lectropol 5):

Mode	POLISHING/ETCHING	Results of Scanned surface
Area	0,5 cm^2	POLISHING
Temp	22°C	20V
Electrolyte	A3	ETCHING
Flow rate	16 (recommended for Ti pure)	14V
Voltage	Variable	
time	variable	

We have set an etching with the values of 14V and 3s using the electrolyte Struers A3. We have used etching because the polarization curve has recommended us and because in general the etching improves the EBSD results. To see the polishing time effect in the quality of polishing, the voltage was set to 20V, voltage recommended by the polarization curve, and we have changed the period of use. To see the polishing voltage effect in the quality of polishing, the time was set to 25s, the best time obtained in the previous experience, and we have changed the voltage (5v, 20V and 45V). Comparing the surface with unpolished, low voltage, optimal voltage and high voltage. When we have applied the electro-polishing method with the SLS sample, the Edge Effect has appeared over its surface:

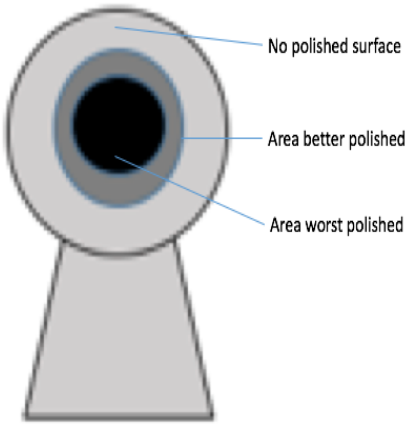

In the Edge Effect the distribution of the electric field is higher in the edges of the surface to be polished than in the centre. So in the edge we found the best polished area. In the middle the oxide layer remains partially recognizable from the cracked morphology. When we clean this area with ethanol we can see a roughness surface. As we will later explain, with high voltages the effect decreases but the surface can broke and shows cracks and pits.[40]

Fig 24. SLS sample surface. Polished areas

EFFECT OF POLISHING TIME: CONSTANT VOLTAGE AND VARIABLE TIME

etching	14V 3s	
Voltage[V]	20 constant	
t[s] 50x	5 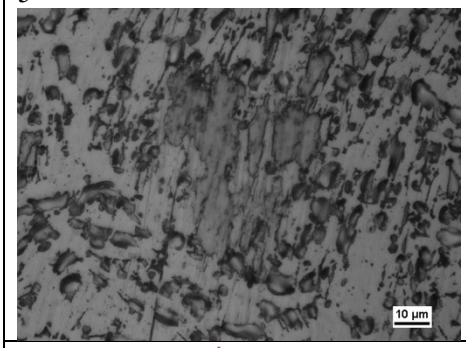	9 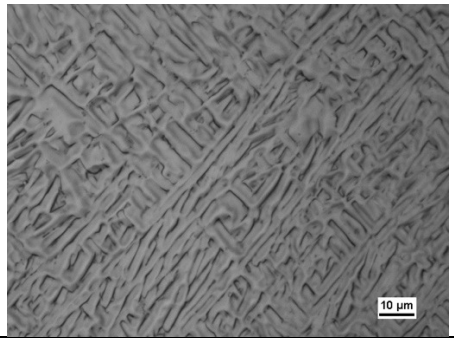
	18 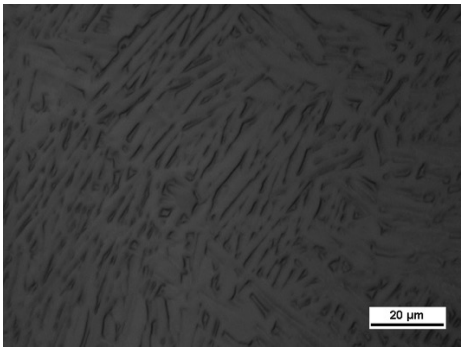	25 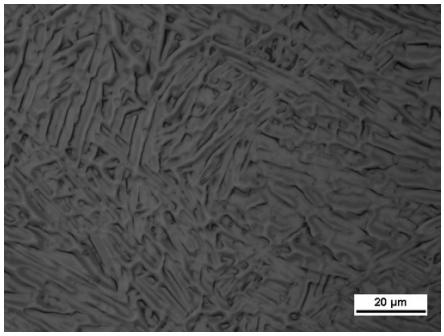
	60 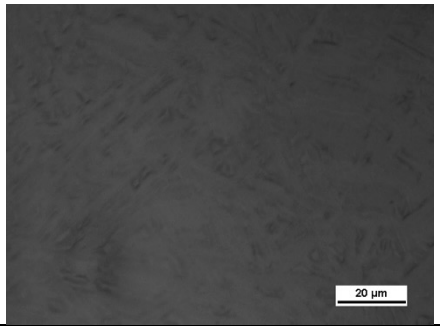	Unpolished 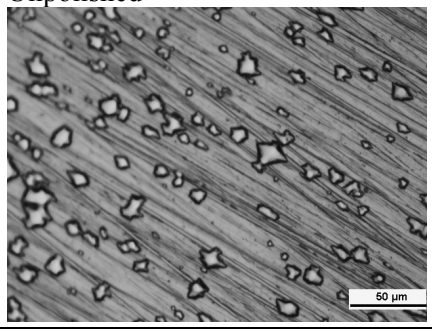

Table 9. Influence of polishing time in surface quality

The table 9 shows the effect of polishing time with the polishing quality. When we apply short time the surface shows a poor quality of polishing. (Fig9 for 5 s). The surface exhibits an incomplete electro-polishing since the oxide layer is not adequately detached.
However, if we increase the time we can see improvements on the polished area. The oxide layer is partially removed from the surface.
With an adequate amount of time for the formation and detachment of oxide layer, we can obtain a good smooth surface.
However, electro-polishing for longer durations like 60s would lead to several pits and cracks formed on the surface. In the image of the table 9 we only have focused a polished area.
In conclusion, when we increase the polishing time until the optimal value (25s), the scratches and roughness are removed from the surface. After this time, if we continue with the polishing we don´t obtain better results. Moreover, if we use long time (60s) the surface presents damages as pits cracks or roughness.[41]
In this research we have used an alloy of titanium, so the dissolution could be favoured in several micro-regions by the formation of galvanic pairs. Two metals in wet electric contact, the noble metal will be less reactive respect to the inert metal. So the material more reactive wears out relatively quickly. In our case the titanium is nobler than the aluminium [42]

VOLTAGE EFFECT STUDY: VARIABLE VOLTAGE AND CONSTANT TIME

<table>
<tr><td>etching</td><td colspan="2">14V 3s</td></tr>
<tr><td>time</td><td colspan="2">25s constant</td></tr>
<tr><td rowspan="4">Voltage[V]</td><td>5V</td><td>45V</td></tr>
<tr><td>2.5x
 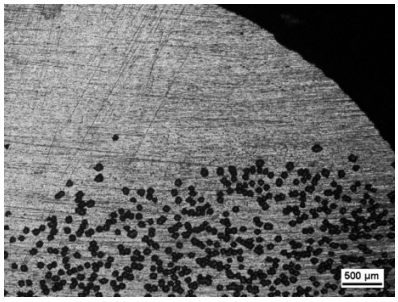 </td><td>2.5x
 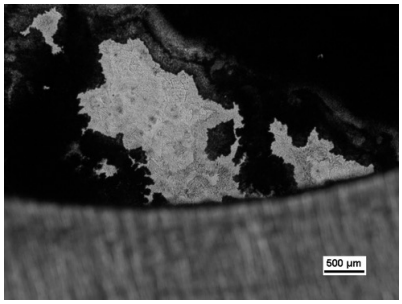 </td></tr>
<tr><td>20x
 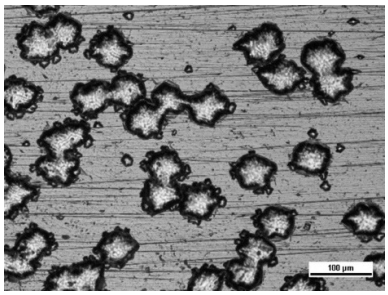 </td><td>50x
 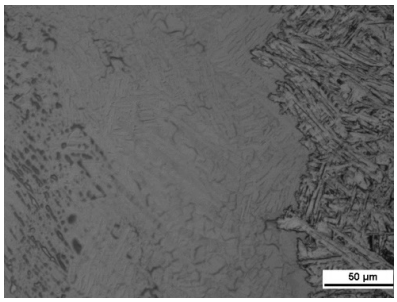 </td></tr>
<tr><td>50x
 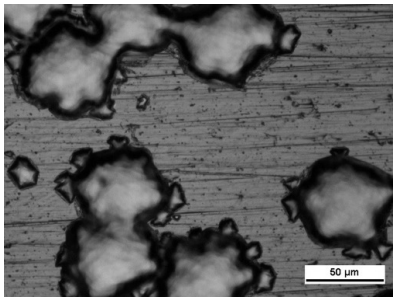 </td><td>100x
 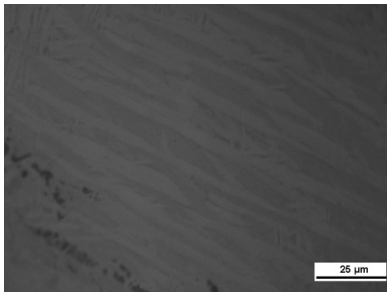 </td></tr>
</table>

Table 10. Influence of polishing Voltage in surface quality

As we can see in the table 10. At low voltage (under 15V), electro-polishing is only effective in areas close to the edges of sample. As we noted earlier, the edge-effect has appeared in the SLS sample. It happens when the electrical field distribution is stronger on the edge of the sample than in its middle area. This, in turn, increases the electro-polishing current. Therefore, the sample is only electro-polished around the corners. In the centre surface of the sample, the oxide layer remained partially on the surface, recognisable from the cracked morphology. However, after the sample was taken out of the electrolyte and rinsed several times with distilled water, the oxide layer was detached and then a rough surface

Below 15 V, an oxide layer is developed with a thickness lower than the critical magnitude. Therefore, it is not detached from the surface using the agitation force of the electrolyte. Electro-polishing at low voltages could not be performed successfully even if the process continues for a longer time

At 20 V, sufficient current is supplied for electro-polishing and a smooth surface was obtained. The sample continues with the edge effect but it is lower.

At higher voltages the situation changes again. Quick detachment of oxide layer was observed at the beginning of experiment. Therefore, the Ti surface was exposed to electrolyte and alternate formation and detachment occurred causing many pits and cracks to develop on the surface. These cracks are macroscopic and can be seen by the naked eye [41]

Other aspect to be considered is the alloy used during the experiments. We haven´t used pure titanium, so in the sample there are different areas with different corrosion resistance. The areas where the allowing elements are weaknesses will suffer more corrosion. [42]

6.3 Electro-polishing parameters to get an optimal polishing.

SLS SAMPLE

The aim of this part is to set the optimal parameters to get the best surface quality by electro-polishing. Actually we only have searched the correct time because the voltage was chosen by the polarization curve. The room temperature was 22ºC, the electrolyte was the Struers A3 and the flow rate 16 was the value recommended by the manufacturer for pure titanium. Then we have realized an etching to get improve the polishing accuracy. By this we have obtained improve the EBSD results. We have set 14V from the polarization curve and 3 seconds to avoid damage the polished surface.

After several test we have obtained an optimal time of 18s to obtain the best surface quality by electro-polishing. The table 11 shows the best polishing surface, of the SLS sample, obtained by electro-polishing using the optimal parameters. The picture 11.a was taken to show the edge effect where the edge of the polished surface is better than the middle. The centre has conserved the protective oxide that has avoided the complete polishing. The pictures 11.b and 11.c show the different polishing areas by different magnification. The picture d is a magnification of the centre where the polishing is worst. By contrast the picture 11.e represents the area close to the edges of the polished surface.

<table>
<tr>
<td rowspan="3">Sample SLS
Polishing paper SiC1200
Paper SiC 2000
Polishing Master Met colloidal Silica=SIO2
Electro-polishing 20V 18s
Etching 14V 3s
Flow rate:16
Area: 0,5
T^a: 22°C
Electrolyte A3</td>
<td>a
 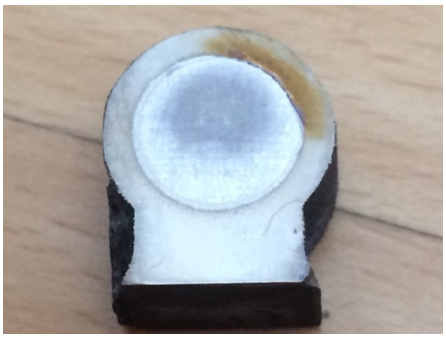 </td>
<td>c 20x
 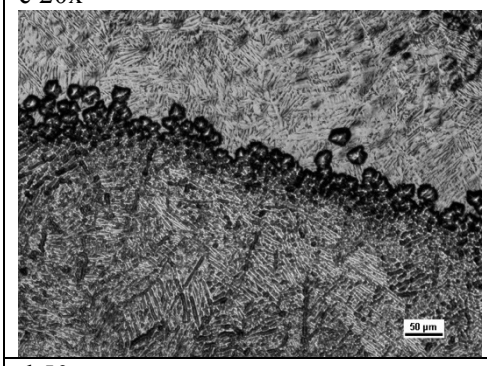
</td>
</tr>
<tr>
<td></td>
<td>d 50x
 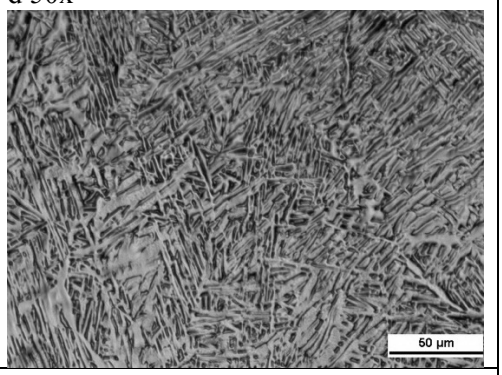
</td>
</tr>
<tr>
<td>b 2.5x
 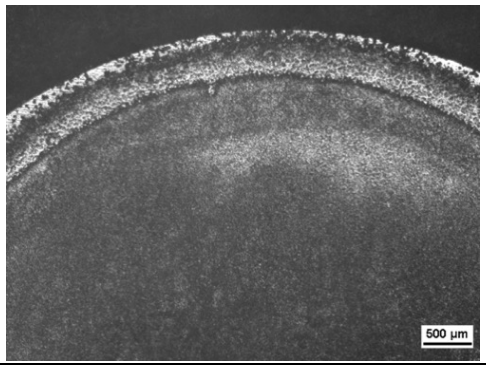
</td>
<td>e 50x
 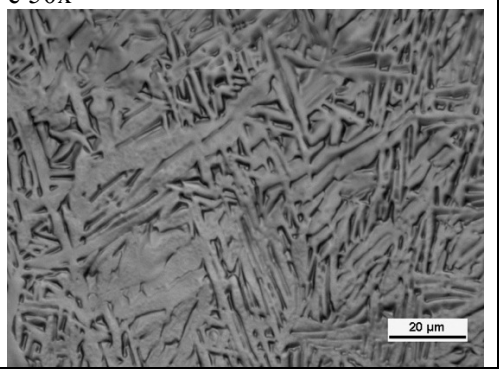
</td>
</tr>
</table>

Table 11. Sample SLS. Optimal polishing with electrolyte

LMpD SAMPLE

Analysis of the LMpD sample after different polishing tests until obtain the best polished surface. The polarization curve has given us the following values about the voltage:

Pulido	etching
20V	0V

So in this case we didn´t applied an etching. Furthermore, the polishing time was shorter than the SLS case. We have applied 20V during 11 seconds because more time involved damages over the surface.

The control parameters to polish the LMpD sample with the best quality possible were:

Sample LMpD Polishing paper SiC1200 SiC 2000 SiC 4000 Polish Master Met coloidal Silica=SIO2 Electropolishing 20V 11s No etching Flow rate:16 Area: 0,5 T^a: 22°C Electrolyte A3	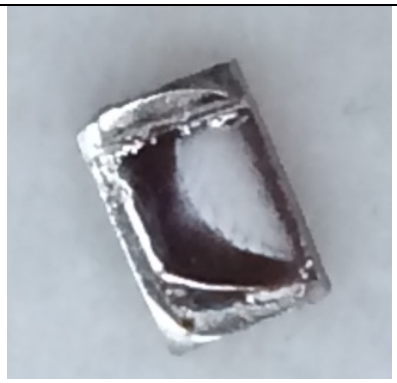 a	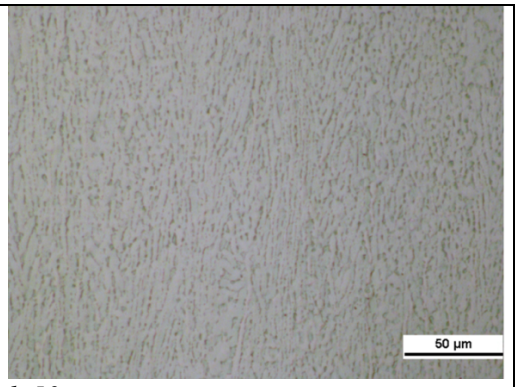 *b 50x*

Table 12. Sample LMpD. Optimal polishing with electrolyte

If we compare the additive manufactured processes observed in this research, the LMpD shows a cooling rate higher than SLS. So the microstructure will be martensite (α´ and α´´)
The martensitic phase is like an α phase but with thin lamellas. This phase is magnetic, with moderate corrosion resistance and high yield strengths A cause of this, the sample showed a high sensitivity with the electro-polishing treatment. For this reason, the oxide layer was dissolved more quickly by the electrolyte. Finally, we have decided not to use the etching and moderate the execution treatment time, 10s. With more time we obtained a damage surface with cracks, pitting and roughness.
It should be noted that the small size of the LMpD sample complicated the work by mechanical polishing. We have tried to use different mounting materials to make ease the polishing process but we didn´t obtain good results by EBSD. We think that the material used didn´t have the enough electric conductivity. As we can see in the figure 25 [43]

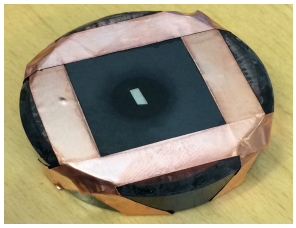

Fig 25. SLS sample mounted with conductive carbon powder and covered with Copper

6.4 Sample analysis by SEM, EBSD:

SLS SAMPLE
SEM: micrograph of the area selected to analyse by electron microscope
By means of slotted corner brackets and bolts we orient the polished surface forming 70º with the horizontal platform into the vacuum chamber. Then, we launch the electron beam over an area previously selected. The main objective is get an area with the best focus possible and where the Backscattered electrons diffract correctly. So we must check the signal intensity captured by the detectors and the focus quality before launching the EBSD analysis. To get it we can play with the SEM parameters to reduce the noise or improve the focusing. The figure 23 has been taken by SEM. It shows the area selected to analyse by EBSD. As we can see, we have obtained a good polishing quality. Over the surface is easily observable the traces of the titanium microstructures

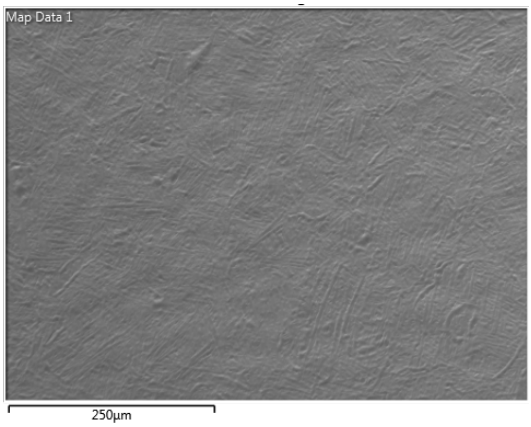

Fig 26 SEM micrograph of surface area from SLS sample

EBSD: orientation and Phases identification in the focused area

One time focused the selected area, we launched the program Aztec activating the SEM detectors; EDS and EBS. This analysis was realized in almost 20 hours, using a normal accuracy, until the system analysed all the selected area points. The software compares the Kikushi bands obtained from the focused area with a data base saved in the computer with several patterns of Kikushi bands. From a reference axis <001>, the system designs the IPF (Pole figure inversion) maps. Where each colour represents the normal vector of the microstructural planes.

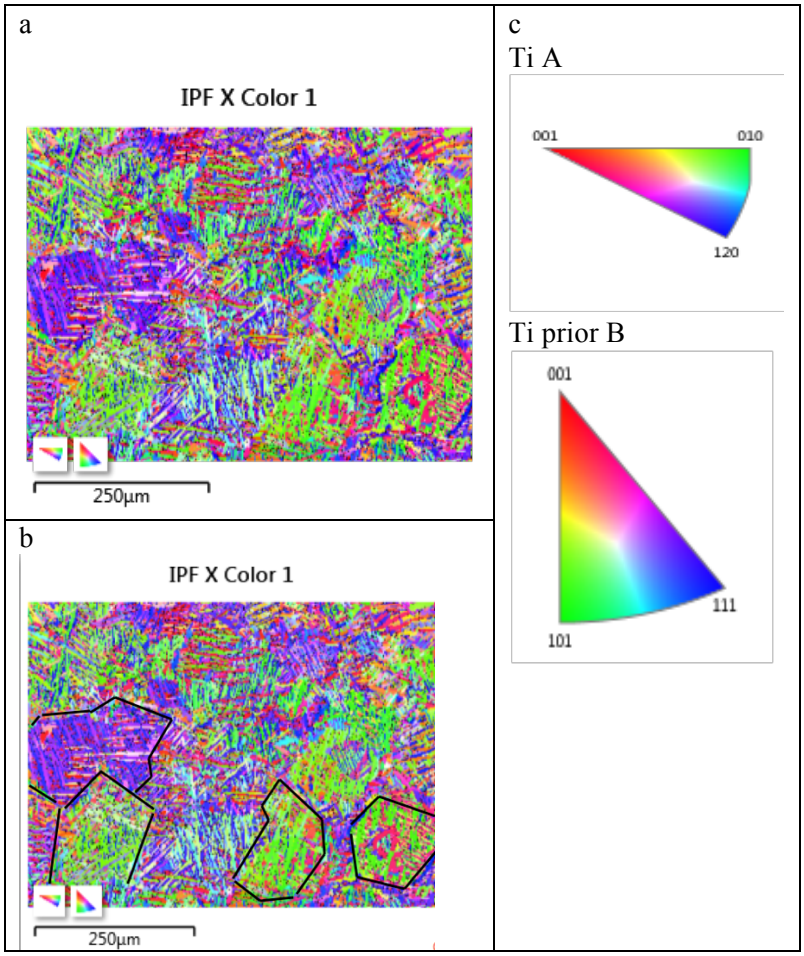

Table 13. IPF of SLS polished area from EBSD results

In the table13.a we can observe α lamellas in prior β grains organized in a basket-weave microstructure. In this case the α lamellas grow up in different directions inside the prior β grains. In the table 13.b we identify the β frontiers. Inside them appear the α lamellas, descendants of the prior β grains. The table 13.c shows the orientation triangles for each phase. They assign a colour

to each orientation. The β triangle is a reconstruction from the α triangle by the Burgers relationship.

LMpD SAMPLE

For the SLS case, we will only analyse the IPF (inverse pole figure) from the EBSD. Because from it we can obtain the most important information related with this project.

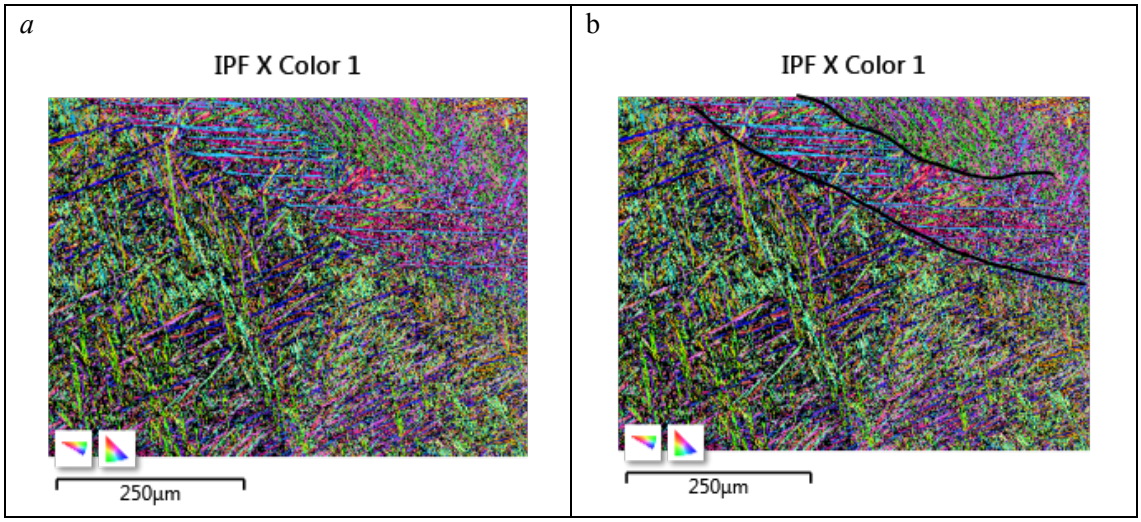

Table 14. IPF of LMpD polished area from EBSD results

As we can see in the table 15a, the LMpD sample shows a martensitic microstructure with huge prior β grains (table15b) growing in the cooling direction. Inside them we found thin lamellas of martensite (α´ and α´´) that grow in the same direction. As we explained, the LMpD is an additive manufactured process with a high cooling rate. This is the cause of the martensitic microstructure. The preparation of the LMpD sample was very tedious due to its small size that complicated the mechanical polishing and the low corrosion of the martensite that complicated the electro-polishing. For these reason we have obtained a polished area with certain damages. Which caused the bad results of the EBSD with a huge proportion of zero solutions.

For futures researches, we recommend apply a reheating or aging treatment over the martensitic sample to improve its behaviour against corrosion. May be with this improvement we could obtain better results with the electro-polishing and the EBSD analysis.

7. CONCLUSIONS

The aim of this projects was to optimise the mechanical and electrolytic polishing parameters to get the best EBSD results analysing two samples made by additive manufactured (SLS and LMpD).

At first, we recommend to prepare the samples with a combination of mechanical and electrolytic polishing to get the best results by EBSD. Beginning with a mechanical polishing with different SiC papers to improve the accuracy (from 1200 to 4000) and then as a final polishing treatment apply the electro-polishing.

The electro-polishing is a final sample preparation step. It cannot be used to remove large quantities of material, so is necessary apply a mechanical polishing first. On the other hand, if we use only the mechanical polishing, we cannot obtain good results with EBSD. This is caused because the mechanical process damages the original crystalline structure by stresses and deformations over the surface.

In the second part of this research, we have evaluated the relation between the polishing time, setting the voltage to the optimal value, and the polishing quality obtained by the electro-polishing process. We recommend use the optimal time to treat the sample. A short time implies an incomplete polishing and a long time causes micro-roughness by the formation of galvanic pairs. We can avoid this defect if we use pure titanium instead of Ti-4V-6Al alloy.

In the third part, we have evaluated the relation between the polishing voltage and the polishing quality of the SLS sample surface, setting constant the time. With low voltage, we obtain a poor polishing quality and the edge effect occurs, the edge of the polished area presents better quality than the centre. We can reduce this effect when the voltage is increased. But if the voltage is too high, the oxide layer cracks in several areas.

In the fourth part, we have tried to set the optimal parameters to get the best EBSD results for the SLS and LMpD samples.

The SLS sample showed a good behaviour with the electro-polishing treatment. After several tests we concluded that the best polishing quality was reached at 20V and 18s with an etching of 14V and 3s.

This sample has a basket-weave microstructure, thick α lamellas growing inside of small β grains in several directions. This results from the fact that SLS process has a high cooling rate (although lower than LMpD)

On the other hand, the LMpD sample was hard to electro-polishing. So we used less time, 20V and 10s, while the etching was impossible to apply because the sample was suffering damages.

This sample shows a martensitic microstructure, thin lamellas of α´ and α´´ (acicular martensite) growing inside and in the same direction (cooling direction) of the huge prior β grains. The martensite is sensitive to the electrolyte application, so the polished surface showed several defects.

In the last part of this research, the samples were analysed by electron microscope SEM and EBSD.

For the reasons discussed, the SLS sample showed better results by EBSD analysis than the LMpD. So its surface is less damaged and the system identified better the microstructural phases.

8. FUTURE WORK

In this point we will talk about the obstacles that we have found during the develop of this research. Moreover, we will suggest possible improvements and alternatives to reach better results.

As stated above, it was very difficult work with the LMpD sample because of its small size, especially during the mechanical polishing. So for futures researches it would be convenient to work with larger samples.

Another option would be mounting the sample with an electrical conductive material to allow the electro-polishing. We tried with conductive carbon powder but we did not obtain good results. With this material the electro-polishing showed several conduction problems even when we added a copper cover.

It would be interesting to analyse the relation between the rest of the control parameters, in electro-polishing, and the polishing quality. Flow rate, electrolyte (e.g. A2), treated area, room temperature.

I would recommend realizing a thermal treatment of reheating or aging with the LMpD sample to improve its corrosion resistance. [45]

Futures researchers could develop this project using samples from other additive manufactured processes.

At last, it would be useful to compare the electro-polishing with other polishing ways such as the chemical etching.

LIST FIGURES

LIST TABLES

REFERENCES

1. Gou Hai-Peng, Zhang Guo-Hua, Kuo-Chih Chou. Preparation of titanium carbide powder from ilmenite concentrate. Chemical Industry and Chemical Engineering Quarterly. 2017;23(1):67-72.

2. Abkowitz S. The emergence of the titanium industry and the development of the ti-6AI-4V alloy. Vol 1. Warrendale, Pa: TMS; 1999.

3. Hanson B. Theœ selection and use of titanium. Vol 641. London: Inst. of Materials; 1995.

4. Ballo A, Xia W, Lindahl C, et al. Early bone tissue responses to a silica-substituted apatite/titanium dioxide coating on titanium implant.2010.

5. Arcella F, Froes F. Producing titanium aerospace components from powder using laser forming. JOM. 2000;52(5):28-30.

6. Boyer R. Materials properties handbook: Titanium alloys. 1. printing ed. Materials Park, OH: ASM Internat; 1994.

7. Nandwana P. Titanium boride formation and its subsequent influence on morphology and crystallography of α precipitates in titanium alloys. University of North Texas; 2013.

8. Danieli C Rodrigues, Pilar Valderrama, Thomas G Wilson, et al. Titanium corrosion mechanisms in the oral environment: A retrieval study. Materials. 2013

9. Schuster J, Palm M. Reassessment of the binary aluminum-titanium phase diagram. JPED. 2006; 255-277

10. Evans M. The θ projection method and small creep strain interpolations in a commercial titanium alloy. Journal of Materials Science. 2001

11. Ti-6Al-4V. Experian Commercial Risk Database. 2017

12. Wang G, Hui S, Ye W, Mi X, Wang Y, Zhang W. Microstructure and tensile properties of low cost titanium alloys at different cooling rate. Rare Met. 2012

13. Matsumoto H, Yoneda H, Fabregue D, Maire E, Chiba A, Gejima F. Mechanical behaviors of Ti–V–(al, sn) alloys with α′ martensite microstructure. Journal of Alloys and Compounds. 2011

14. Estudio de aleaciones de titanio pulvimetalúrgicas con adición de Fe y Cr. Autor: Enrique Herraiz Lalana. Departamento de ciencia e ingeniería de materiales e ingeniería química. Universidad Carlos III Madrid.

15. Additive Manufacturing of Ti-6Al-4V:Relationship between Microstructure, Defects and Mechanical Properties.Autor: Pia Åkerfeldt. Division of Materials Science Department of Engineering Sciences and Mathematics Luleå University of Technology

16. Deckard, C., "Method and apparatus for producing parts by selective sintering", Patente USPTO nº 4863538, filed October 17, 1986, published September 5, 1989

17. Xueyang Chen Lei Yan Wei Li Zhiyuan Wang Frank Liou Joe Newkirk. Effect of powder particle size on the fabrication of ti-6Al-4V using direct laser metal deposition from elemental powder mixture. 2016.348-355

18. Tong J, Bowen CR, Persson J, Plummer A. Mechanical properties of titanium-based Ti–6Al–4V alloys manufactured by powder bed additive manufacture. Materials Science and Technology. 2017;33(2):138-148

19. http://www.3dprinterworld.com/article/efesto-557-enormous-metal-printing-phenomenon (Halterman, 2017)

20. Microstructural Evolution of Ti-6Al-4V Alloy. Author: Leonardo Pelcastre. Luleå University of Technology. 2008

21. Wycisk E, Solbach A, Siddique S, Herzog D, Walther F, Emmelmann C. Effects of defects in laser additive manufactured ti-6Al-4V on fatigue properties. Physics Procedia. 2014:371-378

22. http://www.substech.com/dokuwiki/doku.php?id=electropolishing. Author: Dr. Dmitri Kopeliovich. 2013/2014

23. http://www.inoxidable.com/electropulido.htm. 19-09-2014. Acerind inoxidable S.A

24. Relisys medical devices ltd files patent application for electro-polishing tool for implant devices. Indian Patent News. 2012.

25. GOVZMAN BORIS, BASOL BULENT M, TALIEH HOMAYOUN, ASHJAEE JALAL, FREY BERNARD M, inventorsSystem for electropolishing and electrochemical mechanical polishing. patent US2005133379A1. Jun 23, 2005.

26. Antonini LM, Mielczarski RG, Pigatto C, Müller IL, de Fraga Malfatti C. The influence of the operating parameters of titanium electropolishing to obtain nanostructured titanium surfaces. Materials Science Forum. 2012;727-728

27. https://www.purdue.edu/ehps/rem/rs/sem.htm. Author: Jim Schweitzer. 2014

28. Electron microprobe analysis: Merging of discoveries in physics, chemistry and microscopy, p. 19, departamento de geología, universidad de Wisconsin-Madison.

29. Scanning Electron Microscope Operation. Author: Roger Robbins. 2015. The University of Texas at Dallas.

30. Goulden J, Sitzman S, Larsen K, Jiang H. Multi-scale EBSD and EDS for detection and analysis of spatially rare grains and phases. Microscopy and Microanalysis. 2014;20(S3):982-983

31. Acquisition of a Field Emission Scanning Electron Microscope (FESEM). Author: Susan Swapp, University of Wyoming. 2012

32. Determination of pattern centre in EBSD using the moving-screen technique. Carpenter DA, Pugh JL, Richardson GD, Mooney LR. J Microsc. 2007 Sep;227(Pt 3):246-7.

33. Manufacturing Ultrafine-Grained Ti-6Al-4V Bulk Rod Using Multi-Pass Caliber RollingMetals - Open Access Metallurgy Journal 5(2):777-789 · May 2015

34. Analysis of α and Prior β Structures in Additively Manufactured Ti-6Al-4V. Material Science and Engineering Project Course. Author: Viktor Sandell. January 2017.

35. Provberedningsrummet E281 Manual Sample Preparation. Lars Frisk. Luleå University of Technology. 11 may 2015. https://www.youtube.com/watch?v=xnWhH_DXBUU&t=1498s

36. Safety data sheet for electrolyte A3-I. 28-01-2016.Approved by DHI: Allan Vorup. Struers.

37. Official website of Struers for electropolishing machine Lectropol 5. 2017 Struers http://www.struers.com/Products/Electrolytic-Preparation/Electrolytic-equipment/LectroPol#

38. Analyse Lectropol-5 Struers. April 2014. Matthieu Gerard. https://www.youtube.com/watch?v=-QZavvp94JY&t=84s

39. Electropolishing applications and techniques. Process complements mechanical finishing methods. By: Johnson H. Cutchin Sr. The Tube & Pipe journal. October 27, 2015.

40. The Investigation of Surface Morphology Forming Mechanisms in Electropolishing Process. Shuo-Jen Lee, Yi-Ho Chen, Jung-Chou Hung. 16 October 2012. Department of Mechanical Engineering, Yuan Ze University. Metal Industries Research & Development Centre.

41. Electropolishing behaviour of pure titanium in perchloric acid–methanol–ethylene glycol mixed solution. N-S. Peighambardoust & F. Nasirpouri. 19 Decembre 2013.

42. Nanostructured Surfaces alloy Ti6AI4V. Influence of Electropolishing Time. Caroline Pigatto, Leonardo M. Antonini, Eduardo L. Schneider y Célia F. Malfatti. niversidade Federal do Rio Grande do Sul, Escuela de Ingeniería, Departamento de Metalurgia , Porto Alegre-Brasil. Universidade Feevale, Instituto de Ciencias Exactas y Tecnológicas, Grupo de Investigación en Materiales, Novo Hamburgo, RS-Brasil. Inf. tecnol. vol.23 no.5 La Serena 2012.

43. Provberedningsrummet E281 Hot Mounting SimpliMet. Lars Frisk. Luleå University of Technology. 8 may 2015. https://www.youtube.com/watch?v=uB23hXjWpZM&list=PL9nARBd2NBsYTIrzhsbvk6fwQROcHO0h0&index=3

44. Microstructure and Phase Transformation of Ti-6Al-4V. Robert Pederson. 2002. Department of Applied Physics and Mechanical Engineering Division of Engineering Materials.

45. Heat treating titanium and its alloys. By Matthew J. Donachie Jr.* Consultant Winchester, N.H. HEAT TREATING PROGRESS • JUNE/JULY 2001.

46. R. Wanhill and S. Barter, Fatigue of Beta Processed and Beta Heat-treated 5 Titanium Alloys, SpringerBriefs in Applied Sciences and Technology, DOI: 10.1007/978-94-007-2524-9_2, Ó The Author(s) 2012